Entropy Measures for Transition Matrices in Random Systems

Zhaohui Chen[1], René Meyer[1], and Zhuo-Yu Xian*[1,2]

[1]Institute for Theoretical Physics and Astrophysics and Würzburg-Dresden Cluster of Excellence ct.qmat, Julius-Maximilians-Universität Würzburg, 97074 Würzburg, Germany
[2]Department of Physics, Freie Universität Berlin, Arnimallee 14, DE-14195 Berlin, Germany

Abstract

A transition matrix can be constructed through the partial contraction of two given quantum states. We analyze and compare four different definitions of entropy for transition matrices, including (modified) pseudo entropy, SVD entropy, and ABB entropy. We examine the probabilistic interpretation of each entropy measure and show that only the distillation interpretation of ABB entropy corresponds to the joint success probability of distilling entanglement between the two quantum states used to construct the transition matrix. Combining the transition matrix with preceding measurements and subsequent non-unitary operations, the ABB entropy either decreases or remains unchanged, whereas the pseudo-entropy and SVD entropy may increase or decrease. We further apply these entropy measures to transition matrices constructed from several ensembles: (i) pairs of independent Haar-random states; (ii) bi-orthogonal eigenstates of non-Hermitian random systems; and (iii) bi-orthogonal states in PT-symmetric systems near their exceptional points. Across all cases considered, the SVD and ABB entropies of the transition matrix closely mirror the behavior of the subsystem entanglement entropy of a single random state, in contrast to the (modified) pseudo entropy, which can exceed the bound of subsystem size, fail to scale with system size, or even take complex values.

*Corresponding author: zhuo-yu.xian@fu-berlin.de

Contents

1 Introduction

The quantum information transfer induced by post-selected processes could be described by a non-trace-preserving transition matrix. Consider a bipartite protocol in which Alice and Bob share an entangled state $|\psi_1\rangle_{bc}$. Alice jointly post-selects her systems a and b onto a fixed entangled state $|\psi_2\rangle_{ab}$, inducing a linear transition matrix τ that maps an unknown input state on a to Bob's system c, as illustrated in Fig. 1. Such post-selected transitions arise in diverse contexts, including time-symmetric quantum mechanics [1],

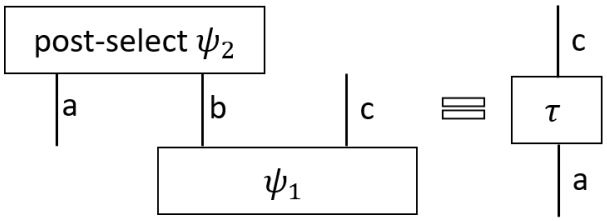

Figure 1: Given an entangled state $|\psi_1\rangle_{bc}$ shared by b and c, the post-selection is performed on the joint system ab with one specific entangled state $|\psi_2\rangle_{ab}$. This operation amounts to transferring the information of an unknown state from a to c via the transition matrix τ.

weak measurement [2, 3], and final-state projection proposals for black hole evaporation [4–7].

Since the associated map $\rho \to \tau\rho\tau^\dagger$ is completely positive but non-trace-preserving, it does not define a quantum channel. So standard fidelity-based measures used in teleportation and CPTP dynamics [8–11] are not applicable. This motivates the use of entropy-based diagnostics to quantify how much information can be transferred through such post-selected processes. Existing proposals include pseudo entropy [12], its modified variants [13], and the SVD entropy [14], each of which captures different structural aspects of the transition matrix but suffers from conceptual or technical limitations.

The pseudo entropy [12] is defined as the von Neumann entropy of the normalized transition matrix $\hat{\tau}$, which is motivated by the entanglement entropy [15, 16] and its holographic duality [17–21]. Since its introduction, pseudo entropy and its extension have been studied in various physical settings, including many-body systems [22, 23], quantum field theories [7, 24–36] and holography [37, 38], and also applied to various phenomena, including timelike entanglement [39–44] and quantum chaos [45–48]. The pseudo entropy of τ constructed from the bi-orthogonal bases of non-Hermitian systems [49] was deeply studied in [50–55]. Especially, in the PT-symmetric SSH model at criticality governed by non-unitary CFT [50], the pseudo entropy displays a logarithmic scaling with a negative central charge. Recently, a modified version of pseudo entropy was proposed by defining the entropy in terms of the logarithm of absolute eigenvalues of $\hat{\tau}$ [13]. The modification avoids the multi-valuedness associated with $\ln\hat{\tau}$ in the pseudo entropy, and can also effectively measure the correct negative central charges in some critical non-Hermitian systems [50, 56] as the pseudo entropy does. Since its introduction, the modified pseudo entropy has been further applied to non-Hermitian quantum systems [57–63], and has also been used to define quantum mutual information in time [64, 65].

However, there are some serious issues associated with the (modified) pseudo entropy. Because the transition matrix is generally non-Hermitian, the resulting entropies can takes negative or complex values rather than being real and positive, and in some cases, may even diverge, exceeding the logarithm of the Hilbert space dimension, e.g., entropy behaviors in PT-symmetric non-Hermitian system [13, 50]. To address these issues, the SVD entropy was introduced in [14], defined as the von Neumann entropy of the SVD-normalized transition matrix $\bar{\tau}$. By construction, the SVD entropy is real, non-negative, and strictly bounded by the logarithm of Hilbert space dimension. Its properties have been further explored in a variety of settings, including general and holographic CFTs and Chern-Simons theory [14], as well as in related applications [66]. In spite of this, some new issues also arise, for example the difficulty of performing field-theoretic calculations due to the presence of the square roots in the definition of $\bar{\tau}$.

Transition matrices	$\hat{\tau}$	$\bar{\tau}$	$\tilde{\tau}$
Normalizations	$\dfrac{\tau}{\mathrm{Tr}\,\tau}$	$\dfrac{\sqrt{\tau^\dagger\tau}}{\mathrm{Tr}\,\sqrt{\tau^\dagger\tau}}$	$\dfrac{\tau}{\sqrt{\mathrm{Tr}\,[\tau\tau^\dagger]}}$
Schmidt coefficients	z_i	q_i	$\sqrt{p_i}$
Spectra for entropy	λ_i	q_i	$p_i\,(\tilde{\tau}\tilde{\tau}^\dagger)$

Table 1: The notation of different normalizations of a given transition matrix τ for (modified) pseudo entropy, SVD entropy and ABB entropy. The normalizations of $\hat{\tau}$ and $\bar{\tau}$ are based on the trace norm, while the normalization of $\tilde{\tau}$ is called state-normalization since we regard $\tilde{\tau}$ as a state between a and c.

Moreover, probabilistic interpretations of pseudo entropy and SVD entropy were proposed in [12,14] by extending the notion of entanglement distillation for pure states [67,68] to the distillation of transition matrices. In this analogy, many copies of an identical transition matrix are asymptotically concentrated into a lower-dimensional one, which is interpreted as distilling a certain number of two-dimensional transition matrices, each contributing an entropy $\ln 2$. In this sense, distillation implies that the associated entropy of a single transition matrix is real, non-negative, and bounded by the dimension of the Hilbert space. Thus, distillation offers a clear and effective description of complicate transition matrices and also reveals the irreversibility of additional non-unitary operations (Sec. 2.3). As in the entanglement distillation, the distillation of transition matrices should admit a clear physically operational interpretation. However, in [12, 14], the so-called probabilities of concentration associated with pseudo entropy and SVD entropy do not correspond to genuine measurement probabilities within the standard quantum mechanics. This motivates us to explore another entropy measure based on distillation that admits a clear probability interpretation.

In this paper, we introduce and analyze the Alter-Brown-Botstein (ABB) entropy, introduced in [69]. The ABB entropy is defined as the von Neumann entropy of $\tilde{\tau}\tilde{\tau}^\dagger$, where $\tilde{\tau}$ denotes a state-normalized transition matrix. Throughout this work, we adopt a notation for transition matrices with different normalizations, as summarized in Tab. 1.

In contrast to the pseudo entropy, modified pseudo entropy, and the SVD entropy, we find that the ABB entropy monotonically decreases under generalized measurements and non-unitary operations, and admits a clear probabilistic interpretation in terms of transition-matrix distillation. We further apply all four entropy measures to Haar random states, non-Hermitian chaotic systems, and the PT-symmetric SYK Lindbladian with linear jump operators [70]. We find that, among these measures, only the SVD entropy and the ABB entropy exhibit physically reasonable behavior as the subsystem size is varied.

The remainder of this paper is organized as follows. In Sec. 2, we introduce the ABB entropy, review the (modified)pseudo entropy and SVD entropy, and analyze the behavior of the different entropies when the transition matrix undergoes generalized measurements and successive quantum operations. In Sec. 3, we discuss the probabilistic interpretations of all four entropy measures based on the distillation of transition matrices. In Secs. 4 and 5, we calculate the ensemble averages of each entropy in the contexts of two Haar random states and non-Hermitian chaotic systems, respectively. In Sec. 6, we analyze the behavior of four entropies in PT-symmetric SYK Lindbladian. Finally, in Sec. 7, we provide concluding remarks and future outlook.

2 Various entropy measures for transition matrices

2.1 Transition matrices from post-selection

As already mentioned in the introduction, we construct the transition matrix τ through post-selection, illustrated in Fig. 1 , and the transition matrix τ is expressed as

$$\tau = \mathrm{Tr}_b \left|\psi_1\right\rangle_{bc} \left\langle\psi_2\right|_{ab} : \mathcal{H}_a \to \mathcal{H}_c \,, \tag{1}$$

which is a linear map from the Hilbert space of system a to that of c. The resulting output state is given up to normalization by

$$\mathrm{Tr}_{ab} \left|\phi\right\rangle_a \left|\psi_1\right\rangle_{bc} \left\langle\psi_2\right|_{ab} = \tau \left|\phi\right\rangle_a \,, \tag{2}$$

with the post-selection probability $(\langle\phi|_a \langle\psi_1|_{bc}) |\psi_2\rangle_{ab} \langle\psi_2|_{ab} (|\phi\rangle_a |\psi_1\rangle_{bc}) = \langle\phi|_a \tau^\dagger\tau |\phi\rangle_a$, where $\tau^\dagger : \mathcal{H}_c \to \mathcal{H}_a$ is the adjoint of τ. For a general mixed state input ρ on system a, the output state up to normalization becomes $\tau\rho\tau^\dagger$, with the corresponding post-selection probability $\mathrm{Tr}[\langle\psi_2|_{ab} (\rho \otimes |\psi_1\rangle_{bc} \langle\psi_1|_{bc}) |\psi_2\rangle_{ab}] = \mathrm{Tr}[\tau\rho\tau^\dagger]$.

Denote the dimensions of $\mathcal{H}_a$, $\mathcal{H}_b$, and $\mathcal{H}_c$ by d_a, d_b, and d_c, respectively. We apply the Schmidt decomposition to the given states $|\psi_1\rangle_{bc}$, $|\psi_2\rangle_{ab}$, and the transition matrix τ. There exist six orthonormal bases such that

$$|\psi_1\rangle_{bc} = \sum_{i=1}^{d_1} x_i \left|\beta_i\right\rangle_b \left|\gamma_i\right\rangle_c \,, \quad |\psi_2\rangle_{ab} = \sum_{i=1}^{d_2} y_i \left|\alpha_i\right\rangle_a \left|\tilde{\beta}_i\right\rangle_b \,, \tag{3}$$

$$\tau = \sum_{i=1}^{d} z_i \left|\tilde{\gamma}_i\right\rangle_c \left\langle\tilde{\alpha}_i\right|_a \,, \quad \tau^\dagger = \sum_{i=1}^{d} z_i \left|\tilde{\alpha}_i\right\rangle_a \left\langle\tilde{\gamma}_i\right|_c \,, \tag{4}$$

where we denote $d_1 = \min(d_b, d_c)$, $d_2 = \min(d_a, d_b)$ and $d = \min(d_a, d_b, d_c)$, and the coefficients x_i, y_i and z_i are real, non-negative numbers, unique up to re-ordering. We emphasize that τ is constructed by taking the partial trace over b of the bipartite states $|\psi_1\rangle_{bc}$ and $|\psi_2\rangle_{ab}$. Because the dimensions of $|\psi_1\rangle_{bc}$ and $|\psi_2\rangle_{ab}$ can be distinct in general, τ is not necessarily a square matrix. Even in square cases, it is generally non-Hermitian except for some special situations where $|\tilde{\gamma}_i\rangle = \pm |\tilde{\alpha}_i\rangle$ holds for all the indices i with $z_i > 0$.

The vector in these bases is unique up to reordering if its corresponding coefficient is nonzero. In general, the overlap matrix $\langle\tilde{\beta}_i|\beta_j\rangle \neq \delta_{ij}$ up to reordering, which implies that the bases $\{|\gamma_i\rangle\}$ and $\{|\tilde{\gamma}_i\rangle\}$ (and likewise for $\{|\alpha_i\rangle\}$) are distinct. The discussion for distillation of transition matrices in Sec. 3 will simplify in the diagonal case, where $|\beta_i\rangle_b = |\tilde{\beta}_i\rangle_b$. In this case, the transition matrix τ in (4) becomes

$$\tau \overset{\text{diag.}}{=} \sum_{i=1}^{d} z_i \left|\gamma_i\right\rangle_c \left\langle\alpha_i\right|_a \,, \quad z_i \overset{\text{diag.}}{=} x_i y_i \,. \tag{5}$$

The transition matrix τ defines a completely positive but non–trace-preserving map that transfers only partial information of the input state from a to c. As a result, standard fidelity-based measures are not suitable for quantifying the amount of information transferred. Instead, we introduce and compare several entropy measures of the transition matrix τ to quantify the amount of information transferred. In the diagonal case, the entropy measures of τ are directly related to the entanglement distillation of the states $|\psi_1\rangle_{bc}$ and $|\psi_2\rangle_{ab}$. Otherwise, their relation becomes more complicated due to the contribution of the non-identical matrix $\langle\tilde{\beta}_i|\beta_j\rangle$.

2.2 Entropy measures of transition matrix

In this section, we define the ABB entropy to describe the information transfer in the above post-selection process with τ and compare it to other measures of entropy.

2.2.1 ABB entropy

We aim to investigate how much information from the input state ρ on system a is transferred into the normalized output state $\rho_\tau = \tau\rho\tau^\dagger/\mathrm{Tr}[\tau\rho\tau^\dagger]$ via the post-selection process governed by the transition matrix τ. The information transfer from a to c can be quantified by the minimal relative entropy between the input and output states, optimized over all unitary transformation U

$$\min_U S[U\rho_\tau U^\dagger||\rho] = \mathrm{Tr}[\rho_\tau \ln \rho_\tau] - \min_U \mathrm{Tr}[U\rho_\tau U^\dagger \ln \rho], \tag{6}$$

where the relative entropy is defined as $S[\rho||\sigma] = \mathrm{Tr}\left[\rho \ln \rho\right] - \mathrm{Tr}\left[\rho \ln \sigma\right]$. Since unitary operation should not affect the amount of information transferred, we rule it out in the relative entropy by minimization. Clearly, this expression depends on both τ and ρ. To isolate the effect of τ, we focus on the scenario in which the input state is the maximally mixed state (MMS) $\rho^{\max} = \mathbb{I}/d_a$, with $\mathbb{I}$ being the identity matrix in dimension d_a. In this case, the output state becomes

$$\rho_\tau^{\max} = \frac{\tau\rho^{\max}\tau^\dagger}{\mathrm{Tr}[\tau\rho^{\max}\tau^\dagger]} = \frac{\tau\tau^\dagger}{\mathrm{Tr}[\tau\tau^\dagger]} = \tilde{\tau}\tilde{\tau}^\dagger = \sum_{i=1}^{d} p_i \left|\tilde{\gamma}_i\right\rangle_c \left\langle\tilde{\gamma}_i\right|_c, \tag{7}$$

where we introduce a normalization for τ, given by

$$\tilde{\tau} = \frac{\tau}{\sqrt{\mathrm{Tr}[\tau\tau^\dagger]}} = \sum_{i=1}^{d} \sqrt{p_i} \left|\tilde{\gamma}_i\right\rangle_c \left\langle\tilde{\alpha}_i\right|_a, \tag{8}$$

with $p_i = \frac{z_i^2}{\sum_j z_j^2}$ and $\sum_i p_i = 1$. This decomposition in the last step follows from the singular value decomposition of τ in (4). Due to $\ln \rho^{\max} = -\ln d_a \mathbb{I}$, any unitary operation on ρ_τ in (6) leaves the relative entropy invariant. Now, the minimal relative entropy between $\rho_\tau^{\max}$ and $\rho^{\max}$ is

$$\min_U S[U\rho_\tau^{\max}U^\dagger||\rho^{\max}] = \mathrm{Tr}[\rho_\tau^{\max} \ln \rho_\tau^{\max}] + \ln d_a. \tag{9}$$

The first term is the negative von Neumann entropy of the output state $\rho_\tau^{\max}$, which is defined as

$$S_{\mathrm{von}}[\rho_\tau^{\max}] = -\mathrm{Tr}[\tilde{\tau}\tilde{\tau}^\dagger \ln(\tilde{\tau}\tilde{\tau}^\dagger)] = -\sum_{i=1}^{d} p_i \ln p_i = S_{\mathrm{ABB}}[\tau]. \tag{10}$$

The MMS $\rho^{\max}$ has the largest von Neumann entropy $\ln d_a$. After post-selection with transition matrix τ, the information loss is reflected in the decrease of $S_{\mathrm{von}}[\rho_\tau^{\max}]$. A large (small) value of $S_{\mathrm{von}}[\rho_\tau^{\max}]$ indicates that most of the states in $\rho^{\max} = \frac{1}{d_a}\sum_{i=1}^{d_a} \left|\tilde{\alpha}_i\right\rangle_a \left\langle\tilde{\alpha}_i\right|_a$ survive (are eliminated) after post-selection, where we have used the basis $\{|\tilde{\alpha}_i\rangle\}$ coming from the decomposition of τ in (4). In the last equality of (10), we identify that this quantity coincides with the ABB entropy $S_{\mathrm{ABB}}[\tau]$, originally introduced in [69] to quantify

the complexity of genome expression data. The name "ABB" is derived from the initials of the authors of [69], following the convention in [14].

Alternatively, based on the Choi-Jamiołkowski (CJ) isomorphism [71, 72], we can map the transition matrix τ in (4) onto an entangled state $|\tau\rangle = \sum_i^d z_i |\tilde{\gamma}_i\rangle_c |\tilde{\alpha}_i\rangle_a$ on the joint system ca. Thus, the normalization of τ in (8) can be interpreted as the normalization of the state $|\tau\rangle$, allowing the ABB entropy in (10) to be interpreted as the entanglement entropy between system c and a on the state $|\tau\rangle$ after normalization. Finally, the corresponding Rényi ABB entropy of τ is given by

$$S_{\text{ABB}}^{(n)}[\tau] = \frac{1}{1-n} \ln \frac{\text{Tr}[(\tau^\dagger \tau)^n]}{\text{Tr}[\tau^\dagger \tau]^n} = \frac{1}{1-n} \ln \text{Tr}\left[(\tilde{\tau}^\dagger \tilde{\tau})^n\right]. \tag{11}$$

where $\text{Tr}[X]^n$ refers to $(\text{Tr}[X])^n$ by default. Obviously, the ABB entropy and its Rényi version are invariant under the bi-unitary transformations $\tau \to U\tau V$ with arbitrary unitary matrices U and V.

We now review three other notions of entropy defined for the transition matrix τ below, namely the (modified) pseudo entropy [12, 13] and the SVD entropy [14].

2.2.2 (Modified) pseudo entropy

Several attempts have been made to generalize the von Neumann entropy for density matrices to describe the "entropy" of non-Hermitian matrices [73] when systems a and c could be identical. In our paper, when the Hilbert spaces of $\mathcal{H}_a$ and $\mathcal{H}_c$ have the same dimension, given a transition matrix τ in (1), we define a linear map from $\mathcal{H}_a$ to $\mathcal{H}_a$ by teleporting the outcome state $\tau |\phi\rangle_a$ from system c back to system a via the perfect quantum teleportation protocol [8, 9, 74] that teleports the basis state $|\gamma_i\rangle_c$ to $|\gamma_i\rangle_a$. Mathematically, this is equivalent to identifying the system a and system c from the beginning. One considers two states $|\psi_1\rangle_{ab}$ and $|\psi_2\rangle_{ab}$ and defines the linear map as

$$\tau = \text{Tr}_b |\psi_1\rangle_{ab} \langle\psi_2|_{ab} = \sum_{i=1}^d z_i |\tilde{\gamma}_i\rangle_a \langle\tilde{\alpha}_i|_a : \mathcal{H}_a \to \mathcal{H}_a, \tag{12}$$

where we have abused the notation of τ. Actually, Eq. (12) is the original definition of a transition matrix as given in [12].

When $|\psi_1\rangle_{ab} = |\psi_2\rangle_{ab}$, the transition matrix $\tau = \text{Tr}_b |\psi_2\rangle \langle\psi_2|$ is Hermitian, positive semi-definite, and has a unit trace, making it mathematically identical to a reduced density matrix on the system a. However, their physical roles are distinct: a transition matrix describes an operation on an unknown quantum state, while a density matrix represents a quantum state itself. Although one could formally apply the von Neumann entropy, $-\text{Tr}[\tau \ln \tau]$, as done in [12], the physical significance of such an entropy remains unclear, since the interpretation of von Neumann entropy for a density matrix cannot be directly extended to a transition matrix.

When $|\psi_1\rangle_{ab} \neq |\psi_2\rangle_{ab}$, τ is neither Hermitian nor positive semi-definite in general. Consequently, its spectrum may contain negative or complex values, and its trace is not necessarily unity but can instead be negative, complex, arbitrarily small or even vanish. It therefore cannot be regarded as a density matrix. Nevertheless, following [12] and assuming $\text{Tr}\,\tau \neq 0$, one can define a normalized transition matrix

$$\hat{\tau} = \frac{\tau}{\text{Tr}\,\tau} = \sum_{i=1}^d \lambda_i |r_i\rangle \langle l_i|, \tag{13}$$

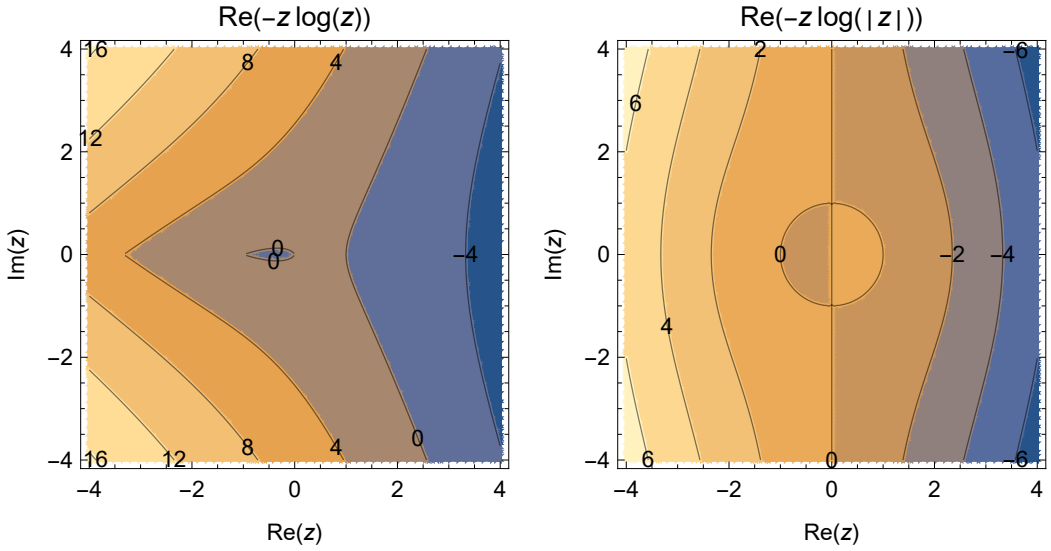

Figure 2: The real parts of two entropy formulas $\mathrm{Re}[-z\ln z]$ and $\mathrm{Re}[-z\ln|z|]$ on the complex plane.

where $\hat{\tau}$ is generally non-Hermitian and thus admits a bi-orthogonal decomposition [49]. The Schmidt bases $\{|\tilde{\gamma}_i\rangle\}$, $\{|\tilde{\alpha}_j\rangle\}$ in (4) are generally not useful in computing the (modified) pseudo entropy, since they are not necessarily bi-orthogonal. The spectrum $\{\lambda_i\}$ is generally complex, and the right and left eigenbasis $\{|r_i\rangle\}$, $\{\langle l_i|\}$ satisfy the bi-orthogonality condition $\langle l_i|r_i\rangle = \delta_{ij}$, $\forall i,\, j$. Substituting the spectrum of $\hat{\tau}$ into the von Neumann and Rényi entropies leads to the definition of the pseudo entropy,

$$S_{\mathrm{P}}[\tau] = -\mathrm{Tr}\left[\hat{\tau}\ln\hat{\tau}\right] = -\sum_{i=1}^{d}\lambda_i\ln\lambda_i, \tag{14}$$

and the Rényi pseudo entropy,

$$S_{\mathrm{P}}^{(n)}[\tau] = \frac{1}{1-n}\ln\mathrm{Tr}\left[\hat{\tau}^n\right] = \frac{1}{1-n}\ln\sum_{i=1}^{d}\lambda_i^n. \tag{15}$$

Since the normalization factor $\mathrm{Tr}\,\tau$ can be negative, complex, arbitrarily small or even vanish, the pseudo entropy may exhibit pathological behavior, including negative or complex values. In particular, as $\mathrm{Tr}\,\tau \to 0$, the pseudo entropy can be strongly amplified or diverge. We will show that it is a common phenomenon near the exceptional points in PT-symmetric non-Hermitian systems in Sec. 6.

For the non-positive spectrum of $\hat{\tau}$, $\ln\hat{\tau}$ in (14) is a multi-valued function, resulting in multi-valued pseudo entropies. In [50], a proper branch of $\ln\hat{\tau}$ was artificially chosen to obtain the desired negative central charge in a non-Hermitian SSH model at a critical point. Complementary to this approach, a modified version of the entropy formula was proposed in [13] as follows [1],

$$S_{\mathrm{MP}}[\tau] = -\mathrm{Tr}\left[\hat{\tau}\ln|\hat{\tau}|\right] = -\sum_{i=1}^{d}\lambda_i\ln|\lambda_i|\,, \tag{16}$$

[1] In general, here the $|\hat{\tau}|$ is different from $\sqrt{\hat{\tau}^\dagger\hat{\tau}}$ nor $\sqrt{\hat{\tau}\hat{\tau}^\dagger}$, except when $\hat{\tau}$ is Hermitian. So the modified pseudo entropy could be considered as a generalization of the FP entropy defined in [64].

where the $|\hat{\tau}|$ is defined by taking the modulus of the spectrum of $\hat{\tau}$ as $|\hat{\tau}| = \sum_{i=1}^{d} |\lambda_i| \times |r_i\rangle \langle l_i|$. This modified definition successfully captures the expected negative central charges in several critical non-Hermitian models [13]. The corresponding Rényi modified pseudo entropy is given by

$$S_{\mathrm{MP}}^{(n)}[\tau] = \frac{1}{1-n} \ln \mathrm{Tr}\left[\hat{\tau}\,|\hat{\tau}|^{n-1}\right] = \frac{1}{1-n} \ln \left(\sum_{i=1}^{d} \lambda_i\,|\lambda_i|^{n-1}\right). \tag{17}$$

The (modified) pseudo entropy and its Rényi version are invariant only under unitary similarity transformations $\tau \to U\tau U^\dagger$. Despite removing logarithmic branch ambiguities, the modified pseudo entropy can still be complex and remains unbounded due to possible small or vanishing $\mathrm{Tr}\,\tau$.

Finally, when dealing with random matrix models, as in Secs. 4 and 5, the ensemble-averaged (modified) pseudo entropy generally reduces to the contribution from the real part, as the imaginary part typically averages out to zero. Given this, we present the value distributions of two entropy formulas $\mathrm{Re}[-z \ln z]$ and $\mathrm{Re}[-z \ln |z|]$ on the complex plane in Fig. 2.

2.2.3 SVD entropy

As mentioned earlier, the pseudo entropy generally exhibits nonphysical behavior, such as complex values or divergencies, due to the general non-positivity or complex nature of the spectrum of τ. To address these issues, a natural alternative to pseudo entropy is the SVD entropy [14], which is based on the singular value decomposition (SVD) of τ. This approach constructs a normalized transition matrix via SVD-normalization as

$$\bar{\tau} = \frac{\sqrt{\tau^\dagger \tau}}{\mathrm{Tr}\sqrt{\tau^\dagger \tau}} = \sum_{i=1}^{d} q_i\,|\tilde{\alpha}_i\rangle_a \langle\tilde{\alpha}_i|_a\,, \tag{18}$$

where the normalized sequence is defined as $q_i = \frac{z_i}{\sum_i z_i}$, with z_i being singular values of τ in (4). Notably, $\bar{\tau}$ in (18) is formally a density matrix defined on the system a, with the transition information from a to c already being encoded in the sequence $\{q_i\}$. Following [14], we give the definition of SVD entropy of τ as

$$S_{\mathrm{SVD}}[\tau] = -\mathrm{Tr}\left[\bar{\tau} \ln \bar{\tau}\right]. \tag{19}$$

The SVD entropy is real, non-negative, and strictly bounded by the Hilbert space dimension. Nevertheless, no concrete bound exists between the SVD entropy of τ and the corresponding entanglement entropies of two states $|\psi_1\rangle_{bc}$ and $|\psi_2\rangle_{ab}$. For a fixed transition matrix τ, one can show that the ABB entropy is always bounded by the SVD entropy, i.e., $S_{\mathrm{SVD}}[\tau] \geq S_{\mathrm{ABB}}[\tau]$, with the proof given in App. A. We will see in later sections that this inequality is universally satisfied across all quantum models considered in this work. In analogy with entanglement entropy, a Rényi version of the SVD entropy for τ is defined by

$$S_{\mathrm{SVD}}^{(n)}[\tau] = \frac{1}{1-n} \ln \frac{\mathrm{Tr}[\sqrt{\tau^\dagger \tau}^{\,n}]}{\mathrm{Tr}[\sqrt{\tau^\dagger \tau}]^n} = \frac{1}{1-n} \ln \mathrm{Tr}\left[\bar{\tau}^n\right], \tag{20}$$

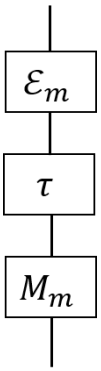

Figure 3: Measurement and non-unitary operation

For convenience in the field-theoretic analysis within the path-integral formalism. An extension of the replica trick is introduced in [14] by incorporating a second replica index m, defined as

$$S_{\rm SVD}^{(n,m)}[\tau] = \frac{1}{1-n} \ln \frac{{\rm Tr}[(\tau^\dagger \tau)^{\frac{mn}{2}}]}{{\rm Tr}[(\tau^\dagger \tau)^{\frac{m}{2}}]^n}, \tag{21}$$

whose value at odd m should be obtained by the analytical continuation of m from even integers due to the fractional powers . The SVD entropy is obtained in the limit

$$S_{\rm SVD} = \lim_{n\to 1} \lim_{m\to 1} S_{\rm SVD}^{(n,m)}. \tag{22}$$

The SVD entropy and its Rényi version are invariant under bi-unitary transformation $\tau \to U\tau V$.

2.3 Entropy monotone

The entanglement transformation is an important topic in quantum information theory, with its connection to majorization established in [75]. Specifically, a bipartite entangled state $|\psi\rangle$ can be transformed into another $|\phi\rangle$ by local operations and classical communication (LOCC) if and only if the spectra of their reduced density matrices satisfy the majorization relation[2] $\lambda_\psi \prec \lambda_\phi$. For the d-dimensional vectors $\lambda_\psi = (x_1, \cdots, x_d)$ and $\lambda_\phi = (y_1, \cdots, y_d)$, each arranged in descending order, $\lambda_\psi \prec \lambda_\phi$ means that [79]

$$\sum_{i=1}^{k} x_i \le \sum_{i=1}^{k} y_i\,, \quad \text{for} \quad k = 1, \cdots, d\,, \tag{23}$$

with equality holding when $k = d$. Since the von Neumann entropy is a Schur-concave function, the majorization relation $\lambda_\psi \prec \lambda_\phi$ implies $S[\lambda_\psi] \ge S[\lambda_\phi]$. In other words, the entanglement entropy of a pure state cannot increase under LOCC. Other entanglement monotonicity under LOCC and also the case of multipartite states were explored in [80–82]. More recently, a LOCC theory for bipartite systems was developed by commuting von Neumann algebras [83], in which the central result states that the LOCC ordering of bipartite pure states is equivalent to the majorization of their restrictions.

[2]Beside the density matrix majorization, one can also discuss the relation between two states in terms of Wigner majorization in the phase space [76–78].

As mentioned in Sec. 2.2.1, since the state-normalized transition matrix $\tilde{\tau}$ corresponds to an entangled state, we explore the analogous relation between local operations, majorization, and entropy transformation for transition matrices in this section.

We consider the transformation from transition matrix $\tilde{\tau}$ to another transition matrix $\tilde{t}$ by first applying a generalized measurement M_m and then applying an operation $\mathcal{E}_m$, as depicted in Fig. 3, where the generalized measurement M_m transformation satisfies $\sum_m M_m M_m^\dagger = I$ and the operation $\mathcal{E}_m$ is a (possibly non-unitary) trace-preserving map depending on the measurement outcome m. The resulting relation between $\tilde{\tau}$ and $\tilde{t}$ is thus given by

$$\tilde{t} \otimes \tilde{t}^\dagger = \sum_m \mathcal{E}_m(\tilde{\tau} M_m \otimes M_m^\dagger \tilde{\tau}^\dagger), \tag{24}$$

where action of $\tilde{t} \otimes \tilde{t}^\dagger$ is to transform any density matrix ρ into $\tilde{t}\,\rho\,\tilde{t}^\dagger$. Analogous to the requirement of the LOCC resulting in pure state [75], here due to the factorized structure on the left-hand side of (24), each term on the right-hand side is proportional to $\tilde{t} \otimes \tilde{t}^\dagger$, i.e., $P_m \tilde{t} \otimes \tilde{t}^\dagger = \mathcal{E}_m(\tilde{\tau} M_m \otimes M_m^\dagger \tilde{\tau}^\dagger)$ with P_m being an undetermined probability constrained by the normalized condition $\sum_m P_m = 1$. Taking the trace over system c, or rather, performing the contraction over the second index of $\tilde{t}$, and using the trace-preserving property of $\mathcal{E}_m$, we obtain

$$P_m \mathrm{Tr}_c[\tilde{t} \otimes \tilde{t}^\dagger] = \mathrm{Tr}_c[\mathcal{E}_m(\tilde{\tau} M_m \otimes M_m^\dagger \tilde{\tau}^\dagger)] \;\Rightarrow\; P_m \tilde{t}^\dagger \tilde{t} = M_m^\dagger \tilde{\tau}^\dagger \tilde{\tau} M_m \,. \tag{25}$$

Applying the polar decomposition [84]

$$M_m^\dagger \sqrt{\tilde{\tau}^\dagger \tilde{\tau}} = \sqrt{M_m^\dagger \tilde{\tau}^\dagger \tilde{\tau} M_m} U_m = \sqrt{P_m} \sqrt{\tilde{t}^\dagger \tilde{t}} U_m, \tag{26}$$

we find

$$\tilde{\tau}^\dagger \tilde{\tau} = \sum_m \sqrt{\tilde{\tau}^\dagger \tilde{\tau}} M_m M_m^\dagger \sqrt{\tilde{\tau}^\dagger \tilde{\tau}} = \sum_m P_m U_m^\dagger \tilde{t}^\dagger \tilde{t} U_m. \tag{27}$$

The eigen spectra of $\tilde{\tau}^\dagger \tilde{\tau}$ and $\tilde{t}^\dagger \tilde{t}$ are denoted by sequences $p[\tilde{\tau}]$ and $p[\tilde{t}]$, respectively. Sorting the elements of both sequences in descending order with $p_i[\tilde{\tau}] \geq p_{i+1}[\tilde{\tau}]$ and $p_i[\tilde{t}] \geq p_{i+1}[\tilde{t}]$, the relation (27) implies the sequences $p[\tilde{\tau}]$ is majorized by $p[\tilde{t}]$, i.e.,

$$p[\tilde{\tau}] \prec p[\tilde{t}]. \tag{28}$$

This is called Nielsen's theorem, whose rigorous proof can be found in [85]. Since the von Neumann entropy $S_{\mathrm{von}}[p] = -\sum_i p_i \ln p_i$ is Schur-concave with respect to the spectrum of p [84], the majorization in (28) ensures that the ABB entropy of τ always decreases under the measurement and non-unitary operation in (24), i.e.,

$$S_{\mathrm{ABB}}[\tau] \geq S_{\mathrm{ABB}}[t]. \tag{29}$$

Next, we examine whether a similar monotonicity holds for the SVD entropy. From (18) and (8), we can easily find that the spectrum of $\bar{\tau}$ can be expressed as $q_i = \frac{\sqrt{p_i}}{\sum_j \sqrt{p_j}}$, which does not necessarily imply $q[\tilde{\tau}] \prec q[\tilde{t}]$, in spite of (28). Now, we can consider a majorization path in the spectrum space $\{p_i\}$, parameterized by the increasing variable s,

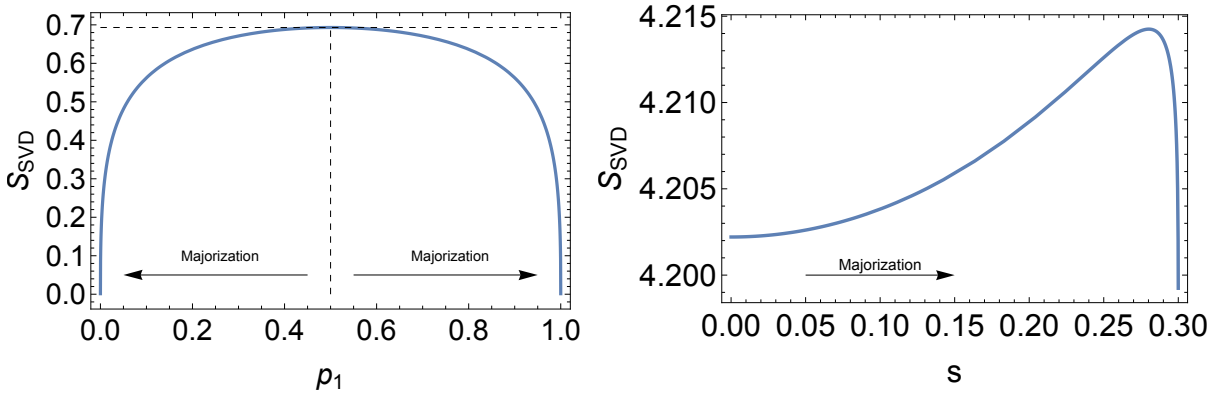

Figure 4: Left: SVD entropy in a two-dimensional Hilbert space. Two majorization paths are shown: one from $p_1 = 0.5$ to 0, and another from $p_1 = 0.5$ to 1 with $p_2 = 1 - p_1$. Along both paths, the SVD entropy decreases monotonically. Right: SVD entropy in an 80-dimensional Hilbert space. Along the majorization path parameterized by $p_1 = 3/10 + s$, $p_2 = 3/10 - s$, and $p_3 = p_4 = \cdots = p_{80} = 1/195$, the SVD entropy increases over a broad range of s.

along which $p[s_1] \succ p[s_2]$ for $s_1 > s_2$. Then we can study how the SVD entropy behaves along the majorization path. The SVD entropy can be expanded as

$$S_{\mathrm{SVD}}[\tau] = -\sum_i q_i \ln q_i = \frac{1}{\sum_j \sqrt{p_j}} \left[-\sum_i \sqrt{p_i} \ln \sqrt{p_i} + \sum_i \sqrt{p_i} \ln \left(\sum_j \sqrt{p_j} \right) \right]. \quad (30)$$

We numerically verify that the SVD entropy is a Schur-concave function of p in low-dimensional Hilbert spaces. For instance, in a two-dimensional Hilbert space, as shown in the left panel of Fig. 4, it decreases monotonically along majorization paths. Similarly, the Schur concavity also holds in three-dimensional space. However, this does not necessarily hold in higher-dimensional Hilbert spaces, such as the majorization path in 80-dimensional Hilbert space shown in the right panel of Fig. 4, the SVD entropy increases along the majorization path in a region, violating the Schur concavity. Moreover, this observation is also confirmed by the Schur-concavity criterion, which states that for any i, j, $\Delta = (p_i - p_j)\left(\frac{\partial S}{\partial p_i} - \frac{\partial S}{\partial p_j}\right) \leq 0$ [86]. Thus, we conclude that the SVD entropy is not universally Schur-concave for the probability distribution $\{p_i\}$ in arbitrary dimensions.

When the (modified) pseudo entropy coincides with the SVD entropy for a Hermitian and positive semi-definite $\hat{\tau}$, the (modified) pseudo entropy also fails to be Schur-concave, as illustrated in Fig. 4. If the (modified) pseudo entropy takes a complex value, the notion of Schur concavity is no longer meaningful. Later, in Sec. 6.1, we will see that in the PT-symmetric region, the (modified) pseudo entropy is real but differs from the SVD entropy. In contrast, since $\tilde{\tau}\tilde{\tau}^\dagger = \bar{\tau} = \mathbb{I}/2$, the ABB entropy, which happens to coincide with the SVD entropy, remains constant. Meanwhile, the pseudo entropy increases as μ decreases, while the modified pseudo entropy decreases with decreasing μ, indicating that neither of them is Schur-concave. In the PT-broken region, the majorization path corresponds to decreasing μ. Along this path, the SVD and ABB entropies decrease monotonically, while the modified pseudo entropy increases. This opposite behavior further confirms that the modified pseudo entropy is not Schur-concave.

In summary, we have demonstrated that transition matrix $\tilde{\tau}$ can be transformed into another transition matrix $\tilde{t}$ via generalized measurement and non-unitary operation if

and only if the spectra of $\tilde{\tau}^\dagger\tilde{\tau}$ and $\tilde{t}^\dagger\tilde{t}$ satisfy the majorization relation $p[\tilde{\tau}] \prec p[\tilde{t}]$, which implies $S_{\mathrm{ABB}}[\tau] \geq S_{\mathrm{ABB}}[t]$. However, this monotonicity does not generally hold for the SVD and pseudo entropies. Therefore, in the context of entropy transformation under LOCC-like operation, the ABB entropy of τ offers a more physically reasonable measure.

3 Probabilistic interpretation

In this section, we will explore the probabilistic interpretation of the ABB entropy from the perspective of distillation. To do that, we first review the entanglement distillation of pure states [67, 68]. Following this perspective, we extend the entanglement distillation from pure states to the transition matrix $\tilde{\tau}$ in (8). Our analysis reveals that only the distillation for the ABB entropy has a well-defined probabilistic interpretation from the construction of the transition matrix. Finally, we revisit the probabilistic interpretation of pseudo entropy [12] and SVD entropy [14], based on the construction of transition matrices $\hat{\tau}$ in (13) and $\bar{\tau}$ in (18). We are unable to find a clear probabilistic interpretation of the pseudo entropy and SVD entropy based on the construction.

3.1 Entanglement distillation of quantum state

The entanglement distillation describes the process of transforming the m-copy entangled states into some amount of EPR pairs through LOCC [67, 68]. In the asymptotic limit $m \to \infty$, the entanglement entropy S in base 2 serves as the asymptotic rate, quantifying the average number of EPR pairs that can be extracted from each copy of the state [87]. We consider the states $|\psi_1\rangle_{bc}$ and $|\psi_2\rangle_{ab}$ in (3). We focus on entanglement distillation from m copies of $|\psi_1\rangle_{bc}$ first, and similarly for $|\psi_2\rangle_{ab}$. Given the Schmidt decomposition of $|\psi_1\rangle_{bc}$ in terms of the d_1 pairs of basis vectors $\{|\beta_i\rangle_b |\gamma_i\rangle_c\}_{i=1}^{d_1}$ in (3), we define a d_1-dimensional subspace spanned by these pairs of basis vectors, namely $\mathcal{H}_1 = \mathrm{span}\{|\beta_i\rangle_b |\gamma_i\rangle_c\}_{i=1}^{d_1}$. The m-copy state $|\psi_1\rangle_{bc}^{\otimes m}$ belongs to the m-copy subspace $\mathcal{H}_1^{\otimes m}$. We further decompose this subspace into the direct sum of $\binom{m+d_1-1}{d_1-1}$ orthogonal subspaces,

$$\mathcal{H}_1^{\otimes m} = \oplus_{\mathbf{k}} \mathcal{H}_{1\mathbf{k}}, \quad \text{with } \mathbf{k} = (k_1, k_2, \cdots, k_{d_1}), \ \sum_{i=1}^{d_1} k_i = m, \tag{31}$$

based on the multinomial expansion $d_1^m = \sum_{\mathbf{k}} d_{1\mathbf{k}}$, where the dimension of the subspace $\mathcal{H}_{1\mathbf{k}}$ is the multinomial coefficient

$$d_{1\mathbf{k}} = \binom{m}{\mathbf{k}} = \frac{m!}{k_1! k_2! \cdots k_{d_1}!}. \tag{32}$$

The number of different configurations of $\mathbf{k}$ is $\binom{m+d_1-1}{d_1-1}$. Accordingly, the state $|\psi_1\rangle_{bc}^{\otimes m}$ can be expressed as a superposition of $\binom{m+d_1-1}{d_1-1}$ MESs $|BC_{\mathbf{k}}\rangle$ over each subspace $\mathcal{H}_{1\mathbf{k}}$,

$$|\psi_1\rangle_{bc}^{\otimes m} = \sum_{\mathbf{k}} \sqrt{P_{1\mathbf{k}}} \, |BC_{\mathbf{k}}\rangle, \ |BC_{\mathbf{k}}\rangle = \frac{1}{\sqrt{d_{1\mathbf{k}}}} \sum_{\mu=1}^{d_{1\mathbf{k}}} \left|B_\mu^{\mathbf{k}}\right\rangle \left|C_\mu^{\mathbf{k}}\right\rangle, \ P_{1\mathbf{k}} = d_{1\mathbf{k}} \prod_{i=1}^{d_1} x_i^{2k_i}, \tag{33}$$

where the state $\left|B_\mu^{\mathbf{k}}\right\rangle$ is a rank-m tensor product of k_1 copies of $|\beta_1\rangle$, k_2 copies of $|\beta_2\rangle$, $\cdots$, k_{d_1} copies of $|\beta_{d_1}\rangle$ for a fixed configuration $\mathbf{k}$, and the index μ labels different orders of these

bases in the tensor product. Similarly, the state $\left|C_\mu^{\mathbf{k}}\right\rangle$ is a tensor product of $\{|\gamma_i\rangle\}$. An incomplete von Neumann measurement projecting onto the subspace $\mathcal{H}_{1\mathbf{k}}$ causes $|\psi_1\rangle_{bc}^{\otimes m}$ to collapse into $|BC_{\mathbf{k}}\rangle$ with probability $P_{1\mathbf{k}}$, as given in (33). The entanglement of a MES, e.g., $|BC_{\mathbf{k}}\rangle$, which has $d_{1\mathbf{k}}$ equally weighted terms in its Schmidt decomposition, can be equivalently regarded as that of $\log_2 d_{1\mathbf{k}}$ EPR pairs.

In the limit $m \to \infty$, the incomplete von Neumann measurement causes the initial state to collapse into the dominant term with highest probability among all $\binom{m+d_1-1}{d_1-1}$ MESs. From Stirling's approximation $m! \approx \sqrt{2\pi m}\,(m/e)^m$ and $k_i! \approx \sqrt{2\pi k_i}\,(k_i/e)^{k_i}$ in the large-m and large-k_i limit, the logarithm of $P_{1\mathbf{k}}$ in (33) is approximated as

$$\ln P_{1\mathbf{k}} \approx m \ln m - \sum_{i=1}^{d_1} k_i \ln \frac{k_i}{x_i^2}. \tag{34}$$

To determine $\mathbf{k}^*$ for the most probable distribution $P_{1\mathbf{k}^*}$, we introduce a Lagrange multiplier μ to enforce the constraint $\sum_{i=1}^{d_1} k_i = m$ and define the function

$$\mathcal{F} = \ln P_{1\mathbf{k}} - \mu \left(\sum_{i=1}^{d_1} k_i - m \right). \tag{35}$$

Taking the derivative with respect to any k_i gives

$$\frac{\partial \mathcal{F}}{\partial k_i} = -\ln \frac{k_i}{x_i^2} - \mu - 1 = 0 \implies k_i = x_i^2\, e^{-\mu-1}. \tag{36}$$

Using the constraint on $\mathbf{k}$ again yields $e^{-\mu-1} = m$. Thus, the probability $P_{1\mathbf{k}}$ sharply peaks around $\mathbf{k}^* = \left(mx_1^2, \cdots, mx_{d_1}^2\right)$. Consequently, the MESs $|BC_{\mathbf{k}^*}\rangle$ in dimension $d_{1\mathbf{k}^*}$ are distilled from $|\psi_1\rangle_{bc}^{\otimes m}$. The dimension of the MES offers an interpretation of the entanglement entropy via

$$\lim_{m\to\infty} \frac{\ln d_{1\mathbf{k}^*}}{m} = -\sum_{i=1}^{d_1} x_i^2 \ln x_i^2 = S_1, \tag{37}$$

where $\log_2 d_{1\mathbf{k}^*}$ measures the expected number of 2-dimensional EPR pairs that could be distilled from $|\psi_1\rangle_{bc}^{\otimes m}$ and we have used (32) for $\mathbf{k}_*$ to compute the limit. This equality states that the entanglement entropy of a quantum state equals the logarithm of the dimension of the MES distilled from its infinite copies, normalized by the number of copies.

In the same approach, $|\psi_2\rangle_{ab}^{\otimes m}$ has the similar expansion

$$|\psi_2\rangle_{ab}^{\otimes m} = \sum_{\mathbf{l}} \sqrt{P_{2\mathbf{l}}}\,|AB_{\mathbf{l}}\rangle\,,\ |AB_{\mathbf{l}}\rangle = \frac{1}{\sqrt{d_{2\mathbf{l}}}} \sum_{\mu=1}^{d_{2\mathbf{l}}} \left|A_\mu^{\mathbf{l}}\right\rangle \left|B_\mu^{\mathbf{l}}\right\rangle,\ P_{2\mathbf{l}} = d_{2\mathbf{l}} \prod_{i=1}^{d_2} y_i^{2l_i}, \tag{38}$$

where $\mathbf{l} = (l_1, l_2, \cdots, l_{d_2})$ satisfies the constraint $\sum_{i=1}^{d_2} l_i = m$, and the state $\left|A_\mu^{\mathbf{l}}\right\rangle$ is a tensor product of $\{|\alpha_i\rangle\}$. Likewise, $P_{2\mathbf{l}}$ peaks around $\mathbf{l}^* = \left(my_1^2, \cdots, my_{d_2}^2\right)$, and the $d_{2\mathbf{l}^*}$-dimensional MESs $|AB_{\mathbf{l}^*}\rangle$ are distilled from $|\psi_2\rangle_{ab}^{\otimes m}$. The corresponding relation between the entanglement entropy of $|\psi_2\rangle_{ab}$ and $|AB_{\mathbf{l}^*}\rangle$ is

$$\lim_{m\to\infty} \frac{\ln d_{2\mathbf{l}^*}}{m} = -\sum_{i=1}^{d_2} y_i^2 \ln y_i^2 = S_2. \tag{39}$$

Next, we extend this notion of distillation from pure states to transition matrices.

3.2 Distillation of transition matrices

In this subsection, we analyze the probabilistic interpretation of ABB entropy, (modified) pseudo entropy and SVD entropy from the distillation. Our goal is to demonstrate that the ABB entropy provides a more physically meaningful measure compared to the pseudo entropy and SVD entropy.

3.2.1 ABB entropy

Now we analyze the probabilistic interpretation of the ABB entropy based on the following two distillation methods.

In Sec. 2.2.1, the ABB entropy of τ is identified with the entanglement entropy of the normalized $|\tilde{\tau}\rangle$ between a and c. Following Sec. 3.1, the entanglement distillation of $|\tilde{\tau}\rangle$ can offer an interpretation of the ABB entropy. Via the CJ isomorphism, the m-copy transition matrix $\tilde{\tau}^{\otimes m}$ corresponds to the m-copy state $|\tilde{\tau}\rangle^{\otimes m}$, both of which have the expansion based on (8),

$$\tilde{\tau}^{\otimes m} = \sum_{\mathbf{k}} \sqrt{P_{\mathbf{k}}}\, \tilde{T}_{\mathbf{k}}, \quad \tilde{T}_{\mathbf{k}} = \frac{1}{\sqrt{d_{\mathbf{k}}}} \sum_{\mu=1}^{d_{\mathbf{k}}} |\tilde{C}_{\mu}^{\mathbf{k}}\rangle\langle \tilde{A}_{\mu}^{\mathbf{k}}|, \tag{40}$$

$$|\tilde{\tau}\rangle^{\otimes m} = \sum_{\mathbf{k}} \sqrt{P_{\mathbf{k}}}\, |\tilde{C}\tilde{A}_{\mathbf{k}}\rangle, \quad |\tilde{C}\tilde{A}_{\mathbf{k}}\rangle = \frac{1}{\sqrt{d_{\mathbf{k}}}} \sum_{\mu=1}^{d_{\mathbf{k}}} |\tilde{C}_{\mu}^{\mathbf{k}}\rangle |\tilde{A}_{\mu}^{\mathbf{k}}\rangle, \tag{41}$$

where $\sum_{\mathbf{k}} d_{\mathbf{k}} = d^m$, and similarly, the state $|\tilde{C}_{\mu}^{\mathbf{k}}\rangle$ is a tensor product of $\{|\tilde{\gamma}_i\rangle\}$ and the state $|\tilde{A}_{\mu}^{\mathbf{k}}\rangle$ is a tensor product of $\{|\tilde{\alpha}_i\rangle\}$. The sub transition matrix $\tilde{T}_{\mathbf{k}}$ defines a rank-$d_{\mathbf{k}}$ isometric map from a to c. Based on (8), (33) and (38), the probability $P_{\mathbf{k}}$ of distilling MES $|\tilde{C}\tilde{A}_{\mathbf{k}}\rangle$ from $|\tilde{\tau}\rangle^{\otimes m}$ can be written as

$$P_{\mathbf{k}} = d_{\mathbf{k}} \prod_{i=1}^{d} p_i^{2k_i} \overset{\text{diag.}}{=} \frac{P_{1\mathbf{k}} P_{2\mathbf{k}}/d_{\mathbf{k}}}{\sum_{\mathbf{j}} P_{1\mathbf{j}} P_{2\mathbf{j}}/d_{\mathbf{j}}}. \tag{42}$$

We observe that in the diagonal case, $P_{\mathbf{k}}$ can be expressed as the joint probability $P_{1\mathbf{k}}P_{2\mathbf{k}}$ of simultaneously distilling $d_{\mathbf{k}}$-dimensional MESs $|BC_{\mathbf{k}}\rangle$ from $|\psi_1\rangle_{bc}^{\otimes m}$ and $|AB_{\mathbf{k}}\rangle$ from $|\psi_2\rangle_{ab}^{\otimes m}$ with a suppression factor $1/d_{\mathbf{k}}$, where the factor accounts for the probability arising from the projection onto the subspace spanned by $\left\{\left|B_{\mu}^{\mathbf{k}}\right\rangle\right\}_{\mu=1}^{d_{\mathbf{k}}}$ during post-selection from $|BC_{\mathbf{k}}\rangle$ to $|AB_{\mathbf{k}}\rangle$. According to the same entanglement distillation process as described in Sec. 3.1, $|\tilde{\tau}\rangle^{\otimes m}$ concentrates on the state $|CA_{\mathbf{k}^*}\rangle$ with the highest probability $P_{\mathbf{k}^*}$ with $\mathbf{k}^* = (mp_1^2, \cdots, mp_d^2)$ in the large-m limit. Correspondingly, the transition matrix $\tilde{\tau}$ also concentrates on the sub transition matrix $\tilde{T}_{\mathbf{k}^*}$ with probability $P_{\mathbf{k}^*}$. Thus, based on the same observation,

$$\lim_{m\to\infty} \frac{\ln d_{\mathbf{k}^*}}{m} = -\sum_{i=1}^{d} p_i \ln p_i = S_{\text{ABB}}[\tau], \tag{43}$$

we find that the ABB entropy of a transition matrix equals the logarithm of the rank of the isometric map distilled from its infinite copies, normalized by the number of copies.

We can give another interpretation of ABB entropy of τ based on the fact that it equals the von Neumann entropy of the output state $\rho_{\tau}^{\max}$ in (7). This entropy equality

implies that the transition matrix $\tilde{\tau}^{\otimes m}$ inherits the distillation process from $(\rho_\tau^{\max})^{\otimes m}$. Based on (7), we have the expansion

$$(\rho_\tau^{\max})^{\otimes m} = \sum_{\mathbf{k}} P_{\mathbf{k}} \rho_{\mathbf{k}}^{\max}, \quad \rho_{\mathbf{k}}^{\max} = \frac{1}{d_{\mathbf{k}}} \sum_{\mu=1}^{d_{\mathbf{k}}} |\tilde{C}_\mu^{\mathbf{k}}\rangle\langle\tilde{C}_\mu^{\mathbf{k}}|, \tag{44}$$

where $\rho_{\mathbf{k}}^{\max}$ is the rank-$d_{\mathbf{k}}$ MMS. The probability of collapsing into $\rho_{\mathbf{k}}^{\max}$ is also $P_{\mathbf{k}}$, which is consistent with (42) and results in the same story of concentration on $\rho_{\mathbf{k}^*}^{\max}$ in the large m-limit. Thus, based on (43) again, the ABB entropy of a transition matrix also equals the logarithm of the rank of the MMS distilled from the infinite copies of the output state of the transition matrix given a full-rank maximally mixed input, normalized by the number of copies.

We showed that the ABB entropy of a transition matrix admits a probabilistic interpretation, where the probability in the diagonal case equals the joint probability of entanglement distillation from the constituent states, modulo suppression by post-selection. Next, we will show that the (modified) pseudo and SVD entropies do not admit such a probabilistic interpretation.

3.2.2 Pseudo entropy

To compare with the distillation of $\tilde{\tau}$ for the ABB entropy, we first revisit the distillation of $\hat{\tau}$ for the (modified) pseudo entropy presented in [12] and then comment on its lack of probabilistic interpretation. As discussed in Sec. 2.2.2, the Schmidt bases $\{|\gamma_i\rangle\}, \{|\alpha_j\rangle\}$ are not mutually orthogonal, rendering them unsuitable for direct probabilistic interpretation. To analyze the concentration behavior of $\hat{\tau}^{\otimes m}$, we instead use the diagonalized form of $\hat{\tau}$ as given in (13), expressed in terms of potentially complex coefficients $\{\lambda_i\}$ and a pair of bi-orthogonal bases $\{|r_i\rangle\}, \{|l_i\rangle\}$. Following [12], the m copies $\hat{\tau}^{\otimes m}$ can be expanded as

$$\hat{\tau}^{\otimes m} = \sum_{\mathbf{k}} \Psi_{\mathbf{k}} V_{\mathbf{k}}, \quad \Psi_k = d_{\mathbf{k}} \prod_{i=1}^{d} \lambda_i^{k_i}, \quad V_{\mathbf{k}} = \frac{1}{d_{\mathbf{k}}} \sum_{\mu=1}^{d_{\mathbf{k}}} \left|R_\mu^{\mathbf{k}}\right\rangle \left\langle L_\mu^{\mathbf{k}}\right|, \tag{45}$$

with $\sum_{\mathbf{k}} \Psi_{\mathbf{k}} = 1$, $\left|R_\mu^{\mathbf{k}}\right\rangle$ the tensor product of $\{|r_i\rangle\}$, $\left|L_\mu^{\mathbf{k}}\right\rangle$ the tensor product of $\{|l_i\rangle\}$, and $\operatorname{Tr} V_{\mathbf{k}} = 1$. Thanks for the bi-orthogonality $\left\langle L_\mu^{\mathbf{k}} | R_\nu^{\mathbf{l}} \right\rangle = \delta_{\mathbf{kl}}\delta_{\mu\nu}$, although the sub transition matrix $V_{\mathbf{k}}$ is non-Hermitian in general, its von Neumman entropy coincides with the logarithm of its rank, namely $S_{\text{von}}[V_{\mathbf{k}}] = \ln d_{\mathbf{k}}$.

In general, λ_i takes a complex value, so we cannot identify $\{\Psi_{\mathbf{k}}\}$ as a probability distribution. We may consider the special case of $\lambda_i \geq 0$, $\forall i$ such that $\Psi_{\mathbf{k}} \geq 0, \forall \mathbf{k}$. In this case, the maximum of $\Psi_{\mathbf{k}}$ is attained at $\mathbf{k}^* = (m\lambda_1, \cdots, m\lambda_d)$. In the large-$m$ limit, we observe that the pseudo entropy of $\hat{\tau}^{\otimes m}$ coincides with $S_{\text{von}}[V_{\mathbf{k}^*}]$:

$$\lim_{m\to\infty} \frac{\ln d_{\mathbf{k}^*}}{m} = -\sum_{i=1}^{d} \lambda_i \ln \lambda_i = S_{\text{P}}[\tau], \tag{46}$$

similar to the relation in ABB entropy (43), but their probabilistic interpretations are different. Although the expansion in (45) resembles that of a density matrix decomposition like (44), the former is an expansion of transition matrices, while the latter is an expansion of density matrices. Consequently, the coefficients $\Psi_{\mathbf{k}}$ should be interpreted

as summations of amplitudes rather than probabilities even they are non-negative in this special case. In fact, we have

$$\Psi_{\mathbf{k}} = \sum_{\mu=1}^{d_{\mathbf{k}}} \left\langle L_\mu^{\mathbf{k}} \right| \hat{\tau}^{\otimes m} \left| R_\mu^{\mathbf{k}} \right\rangle \overset{\text{diag.}}{=} \frac{\sqrt{P_{1\mathbf{k}} P_{2\mathbf{k}}}}{\sum_{\mathbf{j}} \sqrt{P_{1\mathbf{j}} P_{2\mathbf{j}}}}. \tag{47}$$

In the last step, we consider the diagonal case together with the condition of Hermitian and positive semi-definite $\hat{\tau}$, namely $|\gamma_i\rangle = |\tilde{\gamma}_i\rangle = e^{i\theta} |\tilde{\alpha}_i\rangle = e^{i\theta} |\alpha_i\rangle$, such that $\Psi_{\mathbf{k}}$ is expressed as the normalized *square root* of the joint probability $P_{1\mathbf{k}} P_{2\mathbf{k}}$, which further emphasizes that Ψ_k is not a conventional probability in the quantum mechanical sense. Furthermore, even $|\Psi_{\mathbf{k}}|^2$ cannot be interpreted as a physical probability, despite being linear in $P_{1\mathbf{k}} P_{2\mathbf{k}}$ and sharing the same extreme point $\mathbf{k}^*$, since it represents the square of the summation of a series of amplitudes rather than a square of single amplitude,

$$|\Psi_{\mathbf{k}}|^2 = \left| \sum_{\mu=1}^{d_{\mathbf{k}}} \left\langle L_\mu^{\mathbf{k}} \right| \hat{\tau}^{\otimes m} \left| R_\mu^{\mathbf{k}} \right\rangle \right|^2. \tag{48}$$

3.2.3 SVD entropy

Finally we revisit the distillation of $\bar{\tau}$ for the SVD entropy presented in [14] and then comment on its lack of probabilistic interpretation, which is similar to the discussion on pseudo entropy.

Following [14], we consider the m copies of $\bar{\tau}$ and expand $\bar{\tau}^{\otimes m}$ as

$$\bar{\tau}^{\otimes m} = \sum_{\mathbf{k}} \Phi_{\mathbf{k}} W_{\mathbf{k}}, \quad \Phi_{\mathbf{k}} = d_{\mathbf{k}} \prod_{i=1}^{d} q_i^{k_i}, \quad W_{\mathbf{k}} = \frac{1}{d_{\mathbf{k}}} \sum_{\mu=1}^{d_{\mathbf{k}}} \left| \tilde{A}_\mu^{\mathbf{k}} \right\rangle \left\langle \tilde{A}_\mu^{\mathbf{k}} \right|. \tag{49}$$

where $W_{\mathbf{k}}$ is a $d_{\mathbf{k}}$-dimensional transition matrix with $\operatorname{Tr} W_{\mathbf{k}} = 1$, and the coefficients $\{\Phi_{\mathbf{k}}\}$ form a normalized distribution, $\sum_{\mathbf{k}} \Phi_{\mathbf{k}} = 1$. In [14], both $\bar{\tau}^{\otimes m}$ and each $W_{\mathbf{k}}$ are treated formally as density matrices, with $\{\Phi_{\mathbf{k}}\}$ interpreted as a probability distribution directly. The maximum of this distribution is attained at $\mathbf{k}^* = (mq_1, \cdots, mq_d)$, and the SVD entropy of $\bar{\tau}^{\otimes m}$ is identified with the von Neumann entropy of $W_{\mathbf{k}^*}$ in the large-m limit

$$\lim_{m\to\infty} \frac{\ln d_{\mathbf{k}^*}}{m} = -\sum_{i=1}^{d} q_i \ln q_i = S_{\text{SVD}}[\tau]. \tag{50}$$

However, $\bar{\tau}^{\otimes m}$ and $W_{\mathbf{k}}$ should be interpreted as transition matrices rather than density matrices, due to the presence of the square root in the construction of $\bar{\tau}$ in (18). This holds even though they are formally Hermitian, positive semi-definite, and normalized to unit trace. Thus, the decomposition of (49) is still an expansion of transition matrices. Consequently, the coefficients $\Phi_{\mathbf{k}}$ should be still interpreted as summations of amplitudes rather than probabilities. In fact, we have

$$\Phi_{\mathbf{k}} = \sum_{\mu=1}^{d_{\mathbf{k}}} \left\langle \tilde{A}_\mu^{\mathbf{k}} \right| \bar{\tau}^{\otimes m} \left| \tilde{A}_\mu^{\mathbf{k}} \right\rangle = d_{\mathbf{k}} \prod_{i=1}^{d} q_i^{k_i} \overset{\text{diag.}}{=} \frac{\sqrt{P_{1\mathbf{k}} P_{2\mathbf{k}}}}{\sum_{\mathbf{j}} \sqrt{P_{1\mathbf{j}} P_{2\mathbf{j}}}}. \tag{51}$$

In the last step, $\Phi_{\mathbf{k}}$ is given by the normalized square root of the joint probability $P_{1\mathbf{k}}P_{2\mathbf{k}}$, which again underscores that Φ_k does not represent a conventional quantum-mechanical probability. In the same way, $|\Phi_{\mathbf{k}}|^2$ cannot be interpreted as a physical probability, despite being linear in $P_{1\mathbf{k}}P_{2\mathbf{k}}$ and sharing the same extreme point $\mathbf{k}^*$, since it represents the square of the summation of a series of amplitudes rather than a square of single amplitude,

$$|\Phi_{\mathbf{k}}|^2 = \left| \sum_{\mu=1}^{d_{\mathbf{k}}} \left\langle \tilde{A}_\mu^{\mathbf{k}} \right| \bar{\tau}^{\otimes m} \left| \tilde{A}_\mu^{\mathbf{k}} \right\rangle \right|^2 . \tag{52}$$

4 Haar random states and Page curves

In this section, we investigate the universal behaviors of several entropy measures for Haar random states. A Haar random state is generated by applying a unitary matrix, drawn from the circular unitary ensemble (CUE), to a fixed reference state. Due to the unitary invariance of the Gaussian unitary ensemble (GUE) measure, the eigenvectors of a GUE matrix are also distributed according to Haar measure. Therefore, any single eigenvector of a GUE matrix is a Haar random state [88–90].

The average subsystem entanglement entropy of Haar random states exhibits a universal dependence on subsystem size, given by $\overline{S} \approx \ln d_a - d_a/2d_b$ for $1 \ll d_a \leq d_b$ (with d_a and d_b exchanged otherwise), where $D = d_a d_b$ is the total Hilbert space dimension. As a function of the subsystem size $\ln d_a$ at fixed D, the entropy increases linearly, reaches a maximum near balanced subsystem sizes, and then decreases linearly, forming the so-called Page curve [91–93]. It has been extensively studied in black hole information paradox [94, 95].

Beyond standard entanglement entropy, the pseudo entropy for two independent Haar random states was shown to have an extensive complex-valued distribution [12], in contrast to the strong concentration of single-state entanglement entropy around the logarithm of Hilbert space dimension. The SVD entropy was later found to exhibit a behavior analogous to the Page curve in [14]. In this section, we evaluate the averages of the modified pseudo entropy and ABB entropy over Haar random states, as well as the pseudo entropy and SVD entropy, and also compare their properties. Considering two independent Haar random states, $|\psi_1\rangle_{bc}$ and $|\psi_2\rangle_{ab}$, which defines a generally non-square transition matrix, we show analytically that in the large dimension limit with fixed proportion $\ln d_a : \ln d_b : \ln d_c$, both the SVD and ABB entropies are dominated by the logarithm of the smallest Hilbert space dimension. We then calculate the averages of all four types of entropies for different subsystem sizes numerically.

As demonstrated in [96], the ensemble-averaged Rényi entropy for a density matrix ρ admits the approximation

$$\overline{S_n[\rho]} = \frac{1}{1-n} \overline{\ln \frac{\mathrm{Tr}\,[\rho^n]}{\mathrm{Tr}\,[\rho]^n}} \approx \frac{1}{1-n} \ln \frac{\overline{\mathrm{Tr}\,[\rho^n]}}{\overline{\mathrm{Tr}\,[\rho]^n}}, \tag{53}$$

where the fluctuation term is significantly suppressed in the large-dimension limit. Consequently, the ensemble averages of the Rényi versions of the SVD entropy (21) and ABB entropy (11) reduce to evaluating the quantities,

$$\overline{\mathrm{Tr}\,[(\tau^\dagger\tau)^n]}\,,\ \overline{\mathrm{Tr}[\tau^\dagger\tau]^n}\,,\ \overline{\mathrm{Tr}[(\tau^\dagger\tau)^{\frac{mn}{2}}]}\,,\ \overline{\mathrm{Tr}[(\tau^\dagger\tau)^{\frac{m}{2}}]^n}. \tag{54}$$

We construct two Haar random states by $|\psi_1\rangle_{bc} = U_{bc}|0\rangle_{bc}$ and $|\psi_2\rangle_{ab} = V_{ab}|0\rangle_{ab}$, where U_{bc} and V_{ab}, sampled independently from two CUEs, are two unitary matrices acting on $\mathcal{H}_{bc}$ and $\mathcal{H}_{ab}$, respectively. The transition matrix is then given by

$$\tau = \mathrm{Tr}_b\left[U_{bc}|0\rangle_{bc}\langle 0|_{ab}V_{ab}^\dagger\right]. \tag{55}$$

We emphasize that the randomness of τ arises from the random states $|\psi_1\rangle_{bc}$ and $|\psi_2\rangle_{ab}$, and that τ should not be regarded as an independent random matrix. The ensemble average in (54), such as the first trace, can be expressed as

$$\overline{\mathrm{Tr}\left[(\tau^\dagger\tau)^n\right]} = \mathrm{Tr}\int_{\mathrm{Haar}}\left(\mathrm{Tr}_b\left[V_{ab}|0\rangle_{ab}\langle 0|_{bc}U_{bc}^\dagger\right]\mathrm{Tr}_b\left[U_{bc}|0\rangle_{bc}\langle 0|_{ab}V_{ab}^\dagger\right]\right)^n dU_{bc}dV_{ab}. \tag{56}$$

To perform the ensemble averages, we use a key result derived from Schur's lemma in [97, 98], which states that for a D-dimensional Haar random state $U|0\rangle$,

$$\overline{(U|0\rangle\langle 0|U^\dagger)^{\otimes k}} = \frac{\sum_{\pi\in S_k}P_\pi}{D(D+1)\cdots(D+k-1)}, \tag{57}$$

where S_k denotes the permutation group of order $|S_k| = k!$, and P_π is the permutation operator with $\pi = \pi(1)\cdots\pi(k)$, defined as $P_\pi|i_1,\cdots,i_k\rangle = |i_{\pi(1)},\cdots,i_{\pi(k)}\rangle$. For the special case with $n = 2$ and $m = 2$, where $S_{\mathrm{SVD}}^{(2,2)}[\tau]$ coincides with $S_{\mathrm{ABB}}^{(2)}[\tau]$, we employ the result of (57) for $k = 2$ to obtain the averages as

$$\overline{\mathrm{Tr}\left[(\tau^\dagger\tau)^2\right]} = \frac{d_ad_b + d_bd_c + d_cd_a + 1}{d_b(d_ad_b+1)(d_bd_c+1)}, \tag{58}$$

$$\overline{\mathrm{Tr}\left[\tau^\dagger\tau\right]^2} = \frac{d_ad_bd_c + d_a + d_b + d_c}{d_b(d_ad_b+1)(d_bd_c+1)}, \tag{59}$$

whose detailed derivation can be found in App. B. The corresponding average of the Rényi ABB entropy for $n = 2$ is thus given by

$$\overline{S_{\mathrm{ABB}}^{(2)}[\tau]} = -\ln\frac{d_ad_b + d_bd_c + d_cd_a + 1}{d_ad_bd_c + d_a + d_b + d_c}. \tag{60}$$

For general n and m, the ensemble averages in (54) may be evaluated using the same method in App. B and the result in (57), or rather, the Weingarten functions in [99–101]. However, exact expressions become increasingly cumbersome as n and m grow. We therefore restrict our presentation to the leading-order contributions

$$\overline{S_{\mathrm{SVD}}^{(n,m)}[\tau]} = \frac{1}{1-n}\ln\frac{d_ad_b^{\frac{mn}{2}}d_c^{\frac{mn}{2}} + d_a^{\frac{mn}{2}}d_bd_c^{\frac{mn}{2}} + d_a^{\frac{mn}{2}}d_b^{\frac{mn}{2}}d_c + \cdots}{d_a^nd_b^{\frac{mn}{2}}d_c^{\frac{mn}{2}} + d_a^{\frac{mn}{2}}d_b^nd_c^{\frac{mn}{2}} + d_a^{\frac{mn}{2}}d_b^{\frac{mn}{2}}d_c^n + \cdots}, \tag{61}$$

where we consider $n > 1$ and $m \geq 2$ since the analytical continuation starts from even m. A similar analysis yields the dominant term of the n-Rényi ABB entropy

$$\overline{S_{\mathrm{ABB}}^{(n)}[\tau]} = \frac{1}{1-n}\ln\frac{d_ad_b^nd_c^n + d_a^nd_bd_c^n + d_a^nd_b^nd_c + \cdots}{d_a^nd_b^nd_c^n + \cdots}, \tag{62}$$

where we consider $n > 1$. In the limit of large dimensions with fixed proportion $\ln d_a : \ln d_b : \ln d_c$, both expressions, (61) and (62) reduce to $\ln\min[d_a, d_b, d_c]$, implying that the

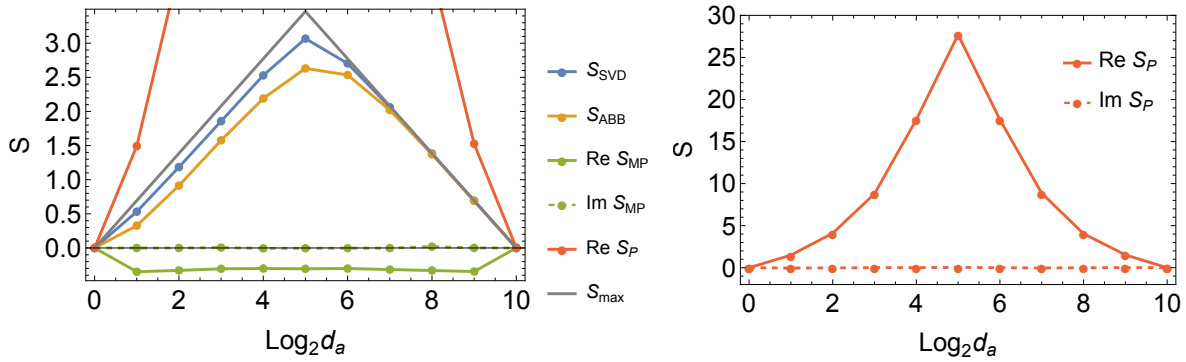

Figure 5: Left: The ensemble averages for the SVD, ABB and (modified) pseudo entropy of the transition matrix in (55), constructed from two independent Haar random states, excluding the imaginary part of pseudo entropy. The gray curve denotes the leading-order term given by (63). Right: Real and imaginary parts of the pseudo entropy. Numerical results are performed over 100 disorder realizations for the SVD and ABB entropies, and 5×10^4 disorder realizations for the (modified) pseudo entropy, under the condition $d_a = d_c$ and $D = d_a d_b = 2^{10}$.

leading-order terms of the averaged Rényi SVD and ABB entropies concentrate around the logarithm of the smallest subsystem's Hilbert space dimension, independent of the Rényi index n. Thus, the averages for the SVD and ABB entropies are respectively dominated by

$$\overline{S_{\rm SVD}[\tau]} = \ln\min\left[d_a, d_b, d_c\right] + \cdots, \quad \overline{S_{\rm ABB}[\tau]} = \ln\min\left[d_a, d_b, d_c\right] + \cdots, \tag{63}$$

where the next-to-leading terms for the averages of two entropies are different.

When identifying a and c, we can consider the (modified) pseudo entropy of τ in (55). Its conjugate transpose, $\tau^\dagger = {\rm Tr}_b[V_{ab}\left|0\right\rangle_{ab}\left\langle 0\right|_{ab}U_{ab}^\dagger]$, is generated from two random states and belongs to the same ensemble as τ, with equal statistical weight. Since the (modified) pseudo entropy of $\tau^\dagger$ is the complex conjugate of that of τ, the ensemble average of the (modified) pseudo entropy is therefore expected to be real.

Substituting τ in (55) into the (modified) pseudo entropy in (14) and (16), SVD entropy in (19), and ABB entropy in (10), respectively, we numerically calculate the ensemble averages of all four types of entropy for varying subsystem sizes $\log_2 d_a$ under the condition $d_a = d_c$ and $d_a d_b = D = {\rm const.}$, as shown in Fig. 5. Our results reproduce the behavior of the average pseudo entropy reported in [12], confirming that the ensemble average of ${\rm Re}\, S_{\rm P}[\tau]$ remains positive while the imaginary part vanishes upon averaging. We find that although the real part exhibits a similar Page curve behavior, it significantly exceeds $\ln d_a$, the maximal value of the entanglement entropy in a Hilbert space of the same dimension. This phenomenon arises from the non-Hermitian nature of the transition matrix $\hat{\tau}$.

To further investigate the origin of this behavior, we analyze the distribution of the spectrum $\{\lambda_i\}$ of $\hat{\tau}$ for the transition matrix τ in (55) over Haar random states, as shown in Fig. 6. We observe that the spectral distribution exhibits approximate rotational symmetry centered around $\bar{\lambda} = 1/d_a$, a consequence of the normalization condition ${\rm Tr}\,\hat{\tau} = \sum_i^{d_a}\lambda_i = 1$. Given that $\bar{\lambda}$ lies on the real axis, the rotational symmetry of the spectrum is consistent with the vanishing of ${\rm Im}\, S_{\rm P}[\tau]$ in the ensemble average. The function ${\rm Re}[-z\,\ln z]$ is positive over more than half of the complex plane, as illustrated in the left panel of Fig. 2. Although the rotationally invariant spectral distribution is slightly

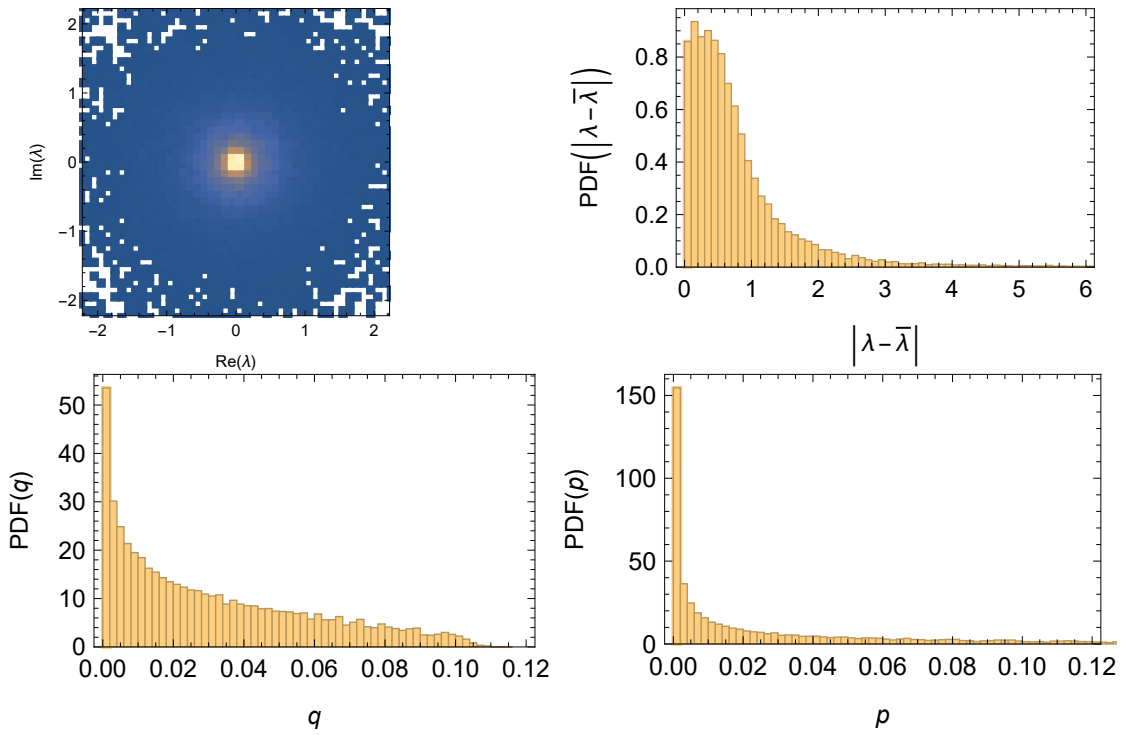

Figure 6: The probability density functions (PDFs) of the eigenvalues $\{\lambda_i\}$ of $\hat{\tau}$, $\{|\lambda_i - \bar{\lambda}|\}$, $\{q_i\}$ of $\bar{\tau}$, and $\{p_i\}$ of $\tilde{\tau}\tilde{\tau}^\dagger$ derived from the transition matrix constructed from two independent Haar random states in (55), over 1000 pairs of disorder realizations at $d_a = d_b = d_c = 2^5$.

shifted along the positive real axis, the majority of the spectrum still lies within the region where $\mathrm{Re}[-z \ln z]$ is positive. Consequently, the ensemble-averaged pseudo entropy S_{P} typically acquires a large positive value for the spectral distribution observed in Fig. 6.

The ensemble-averaged imaginary part of the modified pseudo entropy $\mathrm{Im}\, S_{\mathrm{MP}}[\tau]$ also vanishes, as in the pseudo entropy. In contrast, the real part $\mathrm{Re}\, S_{\mathrm{MP}}[\tau]$ is significantly suppressed and form a stable negative plateau around -0.3, independent of different subsystem sizes. In addition, we observe that both pseudo and modified pseudo entropies in the ensemble average are symmetric with respect to $d_a \leftrightarrow d_b$. This symmetry follows from the fact that τ_a and τ_b, obtained by tracing out the system b and a, respectively, share the same nonzero spectrum. The detailed proof is provided in App. C. Furthermore, we confirm that this negative plateau persists in various total system sizes, including $D = 128$, 256, 512, and 1024.

As shown in the right panel of Fig. 2, the function $\mathrm{Re}[-z \ln |z|]$ is antisymmetric with respect to the imaginary axis. It takes negative values in the right half complex plane ($\mathrm{Re}\, z > 0$), and positive values in the left half plane ($\mathrm{Re}\, z < 0$), except within the unit disk ($|z| \leq 1$), where the sign is reversed. Due to the slight shift of the spectral distribution toward the positive real axis, the portion of the spectrum inside the unit disk contributes positively to $\mathrm{Re}\, S_{\mathrm{MP}}$. However, the spectrum also has a considerable weight outside this unit disk (see PDF of $|\lambda - \bar{\lambda}|$ in Fig. 6), over which the average value of $\mathrm{Re}\, S_{\mathrm{MP}}$ is negative. As a whole, the net negative contribution from outside the unit disk dominates over the positive contribution inside the unit disk. Thus, the ensemble-averaged $\mathrm{Re}\, S_{\mathrm{MP}}$ acquires a small negative value.

Finally, the ensemble-averaged SVD and ABB entropies over two independent Haar

random states exhibit sharp concentration around $\ln \min[d_a, d_b]$, analogous to the Page curve in [91–93]. This is consistent with the analytical prediction (63), because the spectra $\{q_i\}$ of $\bar{\tau}$ and $\{p_i\}$ of $\tilde{\tau}\tilde{\tau}^\dagger$ are confined to the interval $[0, 1]$, similar to conventional entanglement entropy. According to (63), the entropy curves are symmetric under permutations of d_a, d_b and d_c. However, this symmetry is absent when two dimensions coincide, e.g., $d_a = d_c$, and one of $\{d_a, d_b\}$ remains finite. In such a case, the ensemble-averaged SVD and ABB entropies are no longer symmetric with respect to $d_a \leftrightarrow d_b$, as clearly illustrated in Fig. 5, reflecting the fact that $\bar{\tau}_a$ and $\bar{\tau}_b$, as well as $\tilde{\tau}_a\tilde{\tau}_a^\dagger$ and $\tilde{\tau}_b\tilde{\tau}_b^\dagger$, do not share the same nonzero spectrum, which is also explained in App. C. When both d_a and d_b become sufficiently large, the symmetry is approximately restored, which can be verified in the case of $n = 2$ Rényi ABB entropy in Eq. (60). For $d_a < d_b$, the SVD entropy always exceeds the ABB entropy, with both attaining their maxima around $d_a = d_b$. Beyond this point, the two entropies gradually converge as d_a increases. This behavior can be explained by their spectral distributions. As illustrated in Fig. 6, the distribution of $\{p_i\}$ is more concentrated than $\{q_i\}$ due to the quadratic relation $p_i \propto q_i^2$. This concentration is consistent with the majorization relation $q \prec p$, as proven in App. A. Consequently, the ABB entropy is lower than the SVD entropy in the ensemble average.

Thus, we conclude that only the SVD and ABB entropies of the transition matrix, constructed from two independent Haar random states, approach the Page curve in the large-dimension limit, consistent with the subsystem entanglement entropy of a single random state. By contrast, the (modified) pseudo entropy exhibits substantial deviations.

5 Bi-orthogonal eigenstates of non-Hermitian random systems

In the previous section, we examined the behavior of ensemble averages for all four types of entropy associated with the transition matrix τ, constructed from two independent random states. In this section, we turn to the transition matrices constructed from two correlated random states $\langle\psi_1| = \langle L_n|$, $|\psi_2\rangle = |R_n\rangle$, namely

$$\tau = \mathrm{Tr}_b |R_n\rangle \langle L_n| , \tag{64}$$

where $\{\langle L_n|, |R_n\rangle\}$ are taken from the bi-orthogonal basis [49] of a non-Hermitian matrix H of systems a and b defined by

$$H|R_n\rangle = \mathcal{E}_n |R_n\rangle , \quad \langle L_n| H = \mathcal{E}_n \langle L_n| , \quad \mathcal{E}_n \in \mathbb{C} \tag{65}$$

with $\langle L_m|R_n\rangle = \delta_{mn}$, and Tr_b is the partial trace on a subsystem b. In this case, since $|\psi_1\rangle$ and $|\psi_2\rangle$ have the same dimension, the transition matrix τ is square.

We consider the non-Hermitian Hamiltonian H drawn from the Ginibre unitary ensemble (GinUE) or the non-Hermitian SYK model. For such systems, the modified pseudo entropies of the associated transition matrices were studied in [62], revealing a significant suppression of positive values compared to the Page curve of entanglement entropy. Following the analysis in the previous section, we investigate the origin of the plateau values in the bi-orthogonal case by examining the spectral distribution in the ensemble. In this context, we further compute the ensemble averages of the pseudo entropy, ABB entropy, and SVD entropy for varying subsystem sizes and analyze their behaviors from the spectral distribution. Besides, we also explore the universality of our results by analyzing the

non-Hermitian SYK model. We will see that the ABB and SVD entropy of the transition matrices constructed from bi-orthogonal random eigenstates exhibit the behavior of the Page curve, in contrast to the plateau behavior of the modified pseudo entropy discovered in [62].

5.1 Ginibre unitary ensemble

The Hamiltonian of dimension $D \times D$ in the GinUE [102] is defined as $H = \frac{1}{\sqrt{2}}(H_1 + iH_2)$, where H_1 and H_2 are real matrices whose entries are independently sampled from the Gaussian distribution with zero mean value and variance D^{-1}. Here, "unitary" refers to the bi-unitary invariance of the probability density distribution of H under the transformation $H \to UHV$, with U and V being two arbitrary unitary matrices [103]. The GinUE is identified as class A in the Bernard-LeClair symmetry classification [104, 105].

It is well established [102, 106] that in the GinUE, the eigenvalue density follows the circular law in the limit $D \to \infty$; that is, the eigenvalues become uniformly distributed within the unit disk in the complex plane:

$$\rho(w) = \frac{1}{\pi}, \quad \text{for } |w| \leq 1, \quad \text{and otherwise,} \quad \rho(w) = 0, \quad \text{for } |w| > 1.$$

In the large D limit, the spectrum becomes so dense that, given a complex number w with $|w| \leq 1$, one can always find eigenvalues arbitrarily close to w.

At finite D, however, the spectrum is discrete and w need not coincide with any eigenvalue. To identify the closest one, let n_w label the bi-orthogonal eigenstates $\{\langle L_{n_w}|, |R_{n_w}\rangle\}$ whose eigenvalue $\mathcal{E}_{n_w}$ is closest to w in the complex plane. They could be computed by applying the Arnoldi method [107] to the shifted Hamiltonian $H - w$ and selecting the bi-orthogonal eigenstates of the smallest absolute eigenvalue as follows,

$$(H - w)|R_{n_w}\rangle = (\mathcal{E}_{n_w} - w)|R_{n_w}\rangle, \quad \langle L_{n_w}|(H - w) = (\mathcal{E}_{n_w} - w)\langle L_{n_w}|, \tag{66}$$

where $|\mathcal{E}_{n_w} - w|$ is the smallest one among the eigenvaules of H. The transition matrix τ is then constructed by substituting $|R_{n_w}\rangle$ and $\langle L_{n_w}|$ into Eq. (64) as

$$\tau_w = \mathrm{Tr}_b |R_{n_w}\rangle\langle L_{n_w}|. \tag{67}$$

Because H is drawn from the GinUE, the states $|R_{n_w}\rangle$ and $|L_{n_w}\rangle$ are correlated Haar random states, unlike the situation in Sec. 4, where τ was constructed from two independent Haar random states.

Similar to the previous section, since H and $H^\dagger$ belong to the same GinUE, the corresponding transition matrices τ_w and $\tau_w^\dagger$ are drawn from the same ensemble. As a result, both $\mathrm{Im}\, S_{\mathrm{P}}$ and $\mathrm{Im}\, S_{\mathrm{MP}}$ vanish upon ensemble averaging. Figure 7 shows that $\mathrm{Re}\, S_{\mathrm{P}}$ in the ensemble average is also markedly enhanced. This enhancement originates from the fact that the spectral distribution of $\hat{\tau}_w$ derived from (67) in Fig. 8, is largely concentrated in the region where $\mathrm{Re}[-z \ln z]$ remains positive, while the portion of the spectrum lying in the region where $\mathrm{Re}[-z \ln z]$ is negative is very sparse (see Fig. 2).

The real part of the modified pseudo entropy $\mathrm{Re}\, S_{\mathrm{MP}}$ was shown in [62] to be significantly suppressed, forming a plateau in the ensemble average. The plateau value was analytically obtained as

$$\overline{S_{\mathrm{MP}}} = \frac{1 - \gamma - \ln(1 - |w|^2)}{2}, \tag{68}$$

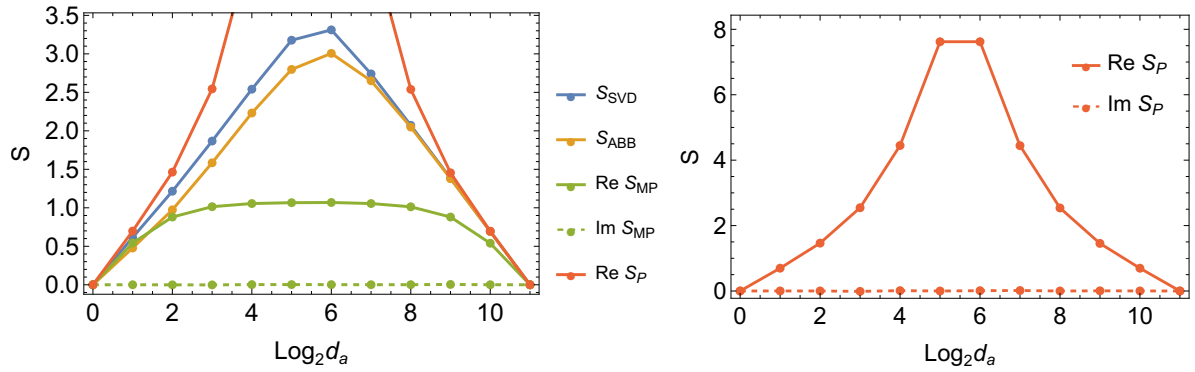

Figure 7: The ensemble averages of the (modified) pseudo entropy, SVD entropy, and ABB entropy of the transition matrix τ_w in (67) constructed from different bi-orthogonal eigenstates of the GinUE matrices with $D = 2^{11}$. The corresponding eigenvalues of the bi-orthogonal eigenstates are $w = |w|\, e^{i\theta}$ and $|w| = 0.9$, with $\theta = k\pi/16$, $k \in 0, \cdots, 31$, and we perform the average over 256 disorder realizations.

in the limit of $1 \ll d_a \ll d_b$, where γ is the Euler-Mascheroni constant. Obviously, this expression is positive and depends only on $|w|$, but remains independent of subsystem dimension d_a and total dimension D. As shown by the green curve in Fig. 7, our numerical results for the modified pseudo entropy at $D = 2^{11}$ reproduce the plateau at $D = 2^{14}$ reported in [62]. In both cases, they match well with this analytical expression (68) even at $d_a = d_b$. To further investigate the origin of the plateau values in the GinUE setting, we analyze the spectral distribution of $\hat{\tau}_w$ again.

As shown in the upper left panel of Fig. 8, the spectral distribution of $\hat{\tau}_w$ is also approximately rotationally invariant around the center $\bar{\lambda} = 1/d_a$. The shift of the center from the origin by $\bar{\lambda}$ results in $\mathrm{Re}\, S_{\mathrm{MP}}$ receiving greater positive contributions from the right half of the unit disk ($\mathrm{Re}\, z > 0$ and $|z| \leq 1$) than negative contributions from the left half ($\mathrm{Re}\, z < 0$ and $|z| \leq 1$), yielding a positive but suppressed value of $\mathrm{Re}\, S_{\mathrm{MP}}$ in the ensemble average. However, unlike the case in Fig. 6, the distribution is concentrated within the disk with a radius less than one. As shown in the upper right panel of Fig. 8, the probability density function of $\left|\lambda - \bar{\lambda}\right|$ peaks in this small region and decays rapidly, approaching zero around $\left|\lambda - \bar{\lambda}\right| \approx 0.8$. This agrees well with the asymptotic result in the large-D limit and under the condition $1 \ll d_a \ll d_b$, as given in [62],

$$\rho(x) = 2x\left(2 - e^{-x^{-2}}\left(2 + 2x^{-2} + x^{-4}\right)\right), \text{ with } x = \frac{\left|\lambda - \bar{\lambda}\right|}{\sqrt{1 - |w|^2}}. \tag{69}$$

Consequently, $\mathrm{Re}\, S_{\mathrm{MP}}$ remains suppressed but positive, although there are negative contributions from outside the unit disk. Its value also depends on $|w|$, as the spectral distribution of $\hat{\tau}_w$ is itself a function of $|w|$.

We further numerically calculate the ensemble averages of the SVD entropy and ABB entropy for τ_w in (67), with the results presented in Fig. 7. The ensemble-averaged SVD and ABB entropies exhibit the same behavior as in the case of two independent Haar random states discussed in Sec. 4. In particular, they are independent of the specific eigenvalue w. As shown in Fig. 8, the distribution of the spectra $\{q_i\}$ and $\{p_i\}$ lies within the interval $[0, 1]$, with $\{p_i\}$ being much more concentrated than $\{q_i\}$ due to the quadratic relation. This behavior again reflects the majorization relation $q \prec p$, and consequently, the SVD entropy is still greater than the ABB entropy in the ensemble average. Finally,

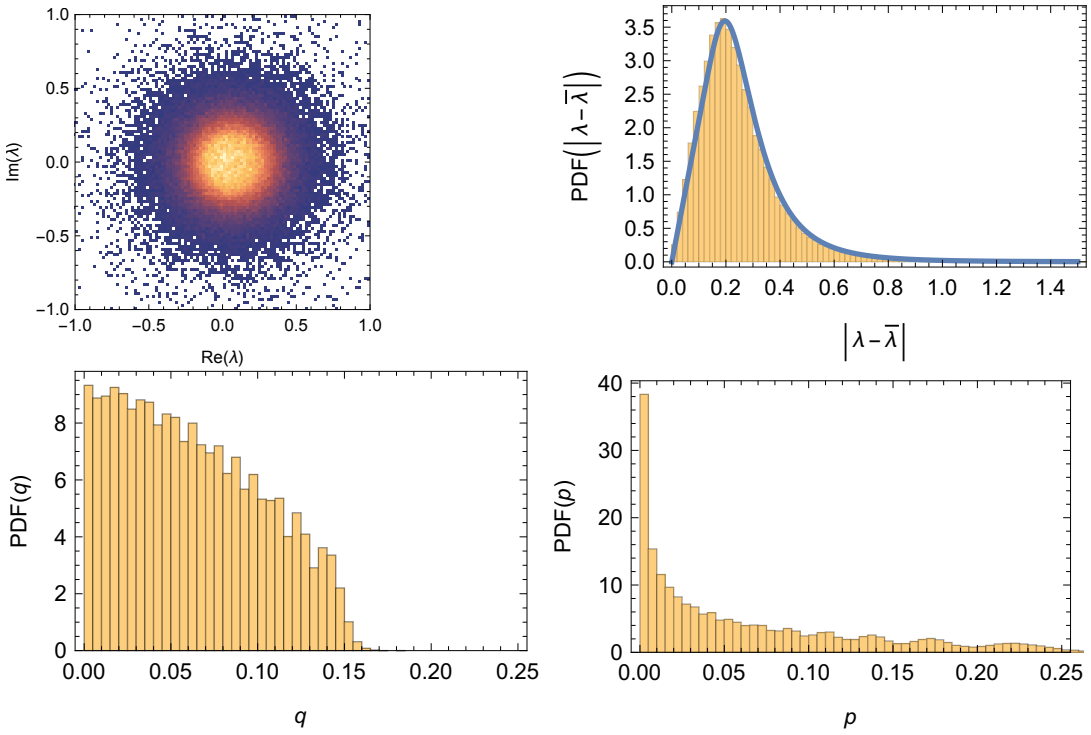

Figure 8: The probability density functions (PDFs) of the eigenvalues $\{\lambda_i\}$ of $\hat{\tau}_w$, $\{|\lambda_i - \bar{\lambda}|\}$, $\{q_i\}$ of $\bar{\tau}_w$, and $\{p_i\}$ of $\tilde{\tau}_w\tilde{\tau}_w^\dagger$, derived from the transition matrix τ_w in (67) constructed from bi-orthogonal eigenstates of GinUE matrices at $d_a = 2^4$ and $d_b = 2^7$. We sample from different eigenstates for $w = |w|\, e^{i\theta}$ and $|w| = 0.9$, with $\theta = k\pi/16$, $k \in 0, \cdots, 31$, and also 256 disorder realizations for each case. The blue curve is given by the analytical result of (69).

we also observe that in the ensemble average, the SVD and ABB entropies are asymmetric under $d_a \leftrightarrow d_b$, while the (modified) pseudo entropy are symmetric. The origin is the same as discussed in the previous section.

The strong suppression of the modified pseudo entropy of the transition matrix constructed from bi-orthogonal bases has been conjectured to be a universal feature of non-Hermitian chaotic many-body systems [62], in contrast to the universal Page curve observed in Hermitian chaotic systems. However, when the spectrum of the transition matrix is complex, we are even unable to identify a probabilistic interpretation of the (modified) pseudo entropy, as discussed in Sec. 3.2.2, let alone relate it to the entanglement of the individual bi-orthogonal eigenstates. In contrast, the SVD and ABB entropies always exhibit a Page-curve-like behavior, even though the bi-orthogonal eigenstates involved are correlated. We therefore propose taking the Page-curves-like behaviors of the ABB or SVD entropies derived from bi-orthogonal eigenstates as features of non-Hermitian chaotic system, consistent with their use in single eigenstates of Hermitian chaotic systems[3]. We will test this proposal in the context of the non-Hermitian SYK model in the next subsection.

[3]Recently, comparisons between the complex-eigenvalue and singular-value spectra of non-Hermitian Hamiltonians and their implications for non-Hermitian chaos have been investigated in [108–113]. Here, we instead focus on the statistics of the entanglement spectrum and the singular-value spectrum of the transition matrix constructed from the bi-orthogonal eigenstates of chaotic and integrable non-Hermitian Hamiltonians.

5.2 Non-Hermitian SYK

The Hermitian SYK model consists of N Majorana fermions $\{\psi_i\}_{i=1}^N$ interacting through all-to-all q-body interactions with real Gaussian-distributed random couplings [114]. For $q = 2$, the model is free and integrable, while for $q \geq 4$, it is chaotic [115]. The entanglement entropy of a subsystem of eigenstates for SYK model was previously studied in [116]. It was shown that when the subsystem size is much smaller than the total system, the entanglement entropy reaches its maximum, i.e., $\ln d_a$. However, for arbitrary q, as d_a increases, the value remains below that of Haar random state, i.e., the Page curve. The rigorous proof of this deviation was provided in [117], indicating that the eigenstates of the SYK model do not fully realize the maximal randomness observed in the Haar random states.

The non-Hermitian SYK (nSYK) model is generalized from the Hermitian SYK model by considering complex random couplings, whose Hamiltonian is [118]

$$H_{\text{nSYK}} = \sum_{1\leq i_1<\cdots<i_q\leq N} \left(J_{i_1\cdots i_q} + iM_{i_1\cdots i_q}\right) \psi_{i_1}\psi_{i_2}\cdots\psi_{i_q}, \tag{70}$$

where $\{\psi_i\}_{i=1}^N$ is a set of Majorana fermion operators satisfying $\{\psi_i, \psi_j\} = \delta_{ij}$. The coupling coefficients $J_{i_1\cdots i_q}$ and $M_{i_1\cdots i_q}$ are both real Gaussian random variables with zero mean and variance $\frac{J^2(q-1)!}{N^{q-1}}$.

We only consider the nSYK of class A in the Bernard-LeClair symmetry classification as well. According to [119, 120], it can be realized in nSYK with $N \mod 8 = 2, 4$ and $q \mod 4 = 0, 2$. The eigen spectrum of nSYK exhibits rotational symmetry in the complex plane, but the eigenvalue distribution is non-uniform, distinct from the GinUE [62, 118].

We construct the transition matrix τ_w according to (67) with the bi-orthogonal eigenstates $|R_{n_w}\rangle$ and $\langle L_{n_w}|$ of nSYK, whose eigenvalue is closest to w. We used the same method of (66) to extract the bi-orthogonal eigenstates and investigate the four types of entropy of the transition matrix τ_w. We numerically investigate the nSYK with $N = 22$ and $q = 2, 4$, which still belongs to class A. To compare the entropies between nSYK with different q, we choose the bi-orthogonal states of eigenvalue w with $w/|E_{\max}|$ being the same, where $|E_{\max}|$ is the maximal absolute eigenvalue. Similar to the case of the GinUE, since the ensemble of H_{nSYK} is the same as its conjugation transpose, the imaginary parts of the averaged entropies vanish, and we focus on their real parts.

At $q = 4$, the averaged entropies as the functions of subsystem size $\log_2 d_a$ are shown in Fig. 9. We observe the following phenomena:

- The pseudo entropy is greatly enhanced.
- The modified pseudo entropy is strongly suppressed and exhibits a plateau, consistent with [62].
- The SVD entropy and the ABB entropy both exhibit a growth-peak-decline behavior. Before reaching their peaks at intermediate system size, the SVD entropy is noticeably larger than the ABB entropy. After the peak, the two entropies gradually converge. Both in their qualitative behavior and in their numerical values, the two entropies of the nSYK model at $q = 4$ are close to those of the GinUE shown in Fig. 7, consistent with the non-Hermitian chaotic nature of the nSYK model at $q = 4$.

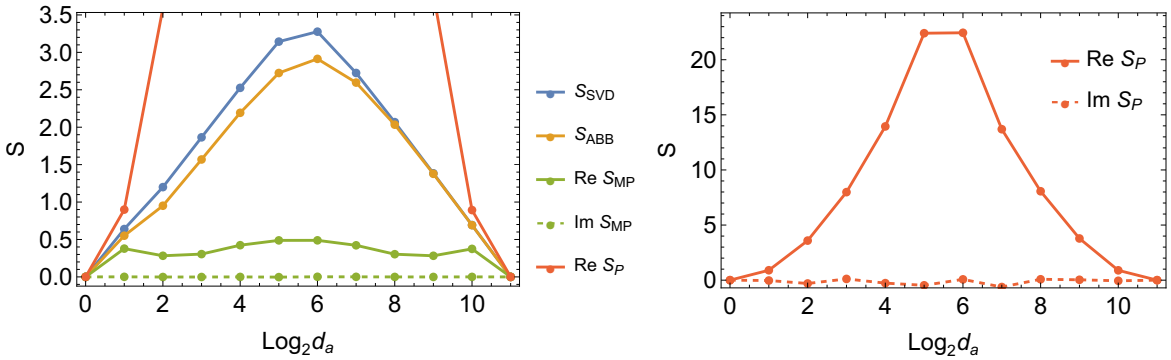

Figure 9: The ensemble averages of the (modified) pseudo entropy, SVD entropy and ABB entropy of the transition matrix τ_w constructed from the bi-orthogonal eigenstates of the non-Hermitian SYK model with $q = 4$, $N = 22$. The corresponding eigenvalues of bi-orthogonal eigenstates are $w = |w|\, e^{i\theta}$, where $|w| \,/\, |E_{\max}| = 0.73$, and $|E_{\max}|$ denotes the maximal absolute eigenvalue. The phase angles are sampled at $\theta = k\pi/16$, with $k \in 0, \cdots, 31$. For each case, we perform average over 512 disorder realizations.

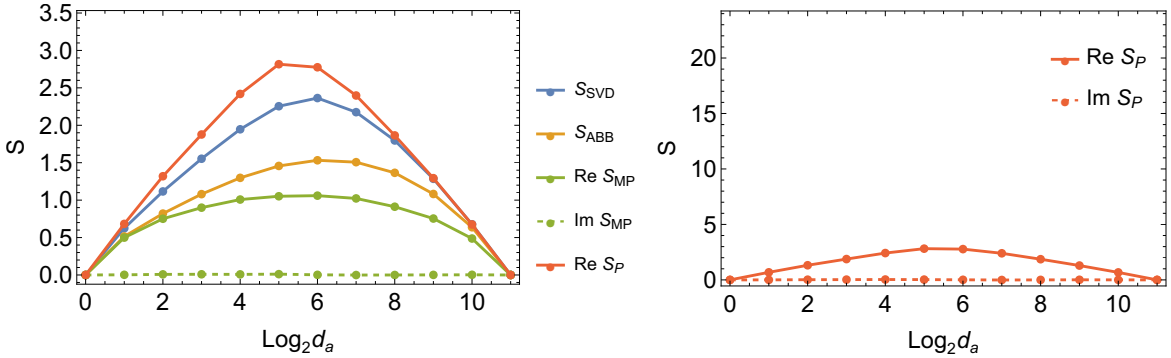

Figure 10: The ensemble averages of the entropies of the transition matrix τ_w constructed from the bi-orthogonal eigenstates of the non-Hermitian SYK model with $q = 2$, $N = 22$. The corresponding eigenvalues of bi-orthogonal eigenstates are $w = |w|\, e^{i\theta}$, where $|w| \,/\, |E_{\max}| = 0.73$. The phase angles are sampled at $\theta = k\pi/16$, with $k \in 0, \cdots, 31$. For each case, we perform average over 512 disorder realizations.

At $q = 2$, the entropies in average as the functions of subsystem size $\log_2 d_a$ are shown in Fig. 10. We observe the following phenomena:

- The pseudo entropy is enhanced as well, but its value is significantly smaller than that at $q = 4$.
- The modified pseudo entropy is suppressed and exhibits a plateau as well, but its value is significantly larger than that at $q = 4$.
- The SVD entropy and the ABB entropy exhibit a growth-peak-decline behavior, but their values are significantly lower than their $q = 4$ counterparts as well as the entropies of the GinUE. We expect that this contrast in entropy values reflects the non-Hermitian chaotic versus integrable properties of the nSYK models, as it parallels the comparison between subsystem entropies of eigenstates in Hermitian SYK models: the entropy at $q = 4$ takes the Page value given by random states and the entropy at $q = 2$ takes a lower value derived by the Wachter law of free

fermions [116]. Moreover, the SVD entropy remains noticeably larger than the ABB entropy, indicating a non-flat singular-value spectrum.

By comparing the entropies from the nSYK at $q = 4$ and $q = 2$, we conclude that

- The enhancement of pseudo entropy is a common feature.
- The suppression and plateau of the modified pseudo entropy of transition matrices constructed in a bi-orthogonal basis are not exclusive for non-Hermitian chaotic systems; the same behaviors can arise even in a free non-Hermitian system.
- The SVD and ABB entropies, computed from bi-orthogonal eigenstates, are sensitive to non-Hermitian chaos, mirroring the sensitivity of eigenstate entanglement entropy to chaos in Hermitian systems.

It would be worthwhile to test these observations in other models in future work.

6 Close to the exceptional point

In this section, we are concerned with the behavior of different entropies when $\mathrm{Tr}[\tau] = \langle\psi_1|\psi_2\rangle$ goes to zero, which occurs in particular at the exceptional points of a PT-symmetric Hamiltonian. We demonstrate that the vanishing of the inner product leads to the divergence of the (modified) pseudo entropy, while the SVD entropy and ABB entropy remain finite.

We begin with a simple PT-symmetric Hamiltonian in a two-qubit system, which serves as an analog of the vectorized Lindbladian studied afterwards. We compute all four entropies for τ, defined in the bi-orthogonal basis. Then we extend our analysis to the SYK Lindbladian.

6.1 Two-qubit system

To further illustrate the distinct behaviors of the above entropy measures, we first consider a simple two-qubit non-Hermitian model, in which two subsystems a and b are coupled as

$$H = iH_a + iH_b + \mu(\sigma_a^x\sigma_b^x + \sigma_a^z\sigma_b^z). \tag{71}$$

where we choose local operators $H_a = \mathrm{diag}(-2/3, 1/3) \otimes \mathbb{I}$ and $H_b = \mathbb{I} \otimes \mathrm{diag}(1/6, 1/6)$ on the system a and b, respectively. The third term describes the interaction between a and b, with μ being a real positive coupling strength and $\sigma^{x,z}$ being Pauli matrices. This toy model shares the similar structure as the vectorized Lindbladian operator (77) discussed later.

We define the unitary operator as $P = \sigma^x \otimes \sigma^x$, and the anti-unitary operator T as complex conjugation. With these definitions, the Hamiltonian H in (71) satisfies PT symmetry. Its eigenvalues are given by

$$E_{1,2} = \pm\mu - \frac{1}{2}\sqrt{4\mu^2 - 1}, \quad E_{3,4} = \pm\mu + \frac{1}{2}\sqrt{4\mu^2 - 1}, \tag{72}$$

as shown in Fig. 11. As μ decreases, each pair of eigenvalues approaches and eventually coalesces at the exceptional point $\mu_c = 1/2$. For $\mu < \mu_c$, the eigenvalues form complex-conjugate pairs. According to PT symmetry properties of non-Hermitian Hamiltonians

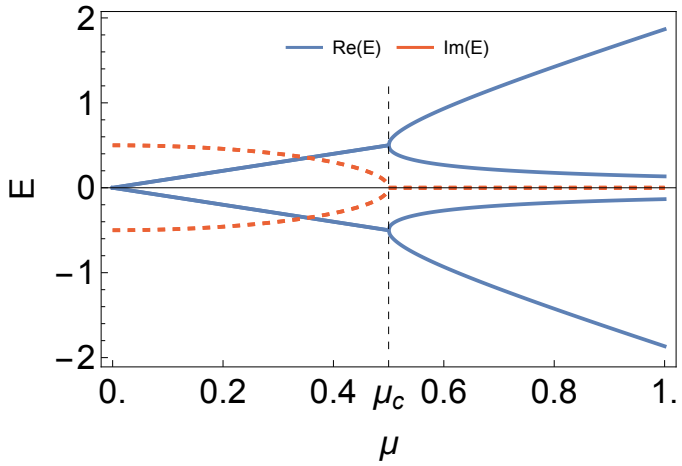

Figure 11: Spectrum of two-qubit model as the function of μ.

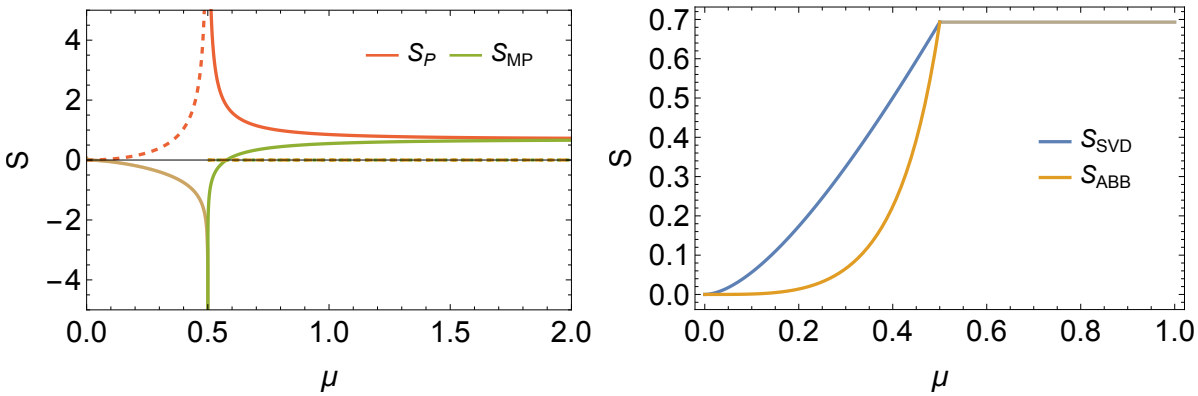

Figure 12: Left: The (modified) pseudo entropy of τ. Solid and dashed lines denote real and imaginary parts, respectively. Their real parts of pseudo entropy and modified pseudo entropy coincide in the PT-broken region. Right: The corresponding SVD and ABB entropies of τ.

discussed in [121,122], the eigenvalues remain real for $\mu > \mu_c$, indicating that PT symmetry of the eigenstates is preserved. For $\mu < \mu_c$, the spectrum becomes complex, signaling that PT symmetry of the eigenstates is broken.

We construct the transition matrix τ from the bi-orthogonal eigenstates. For this model, τ has the same form across all four eigenstates, so we only need to consider one eigenstate. Two distinct expressions of $\hat{\tau}$ corresponding to PT-symmetric and PT-broken regions are obtained as

$$\hat{\tau}_{\mu>\mu_c} = \begin{pmatrix} \frac{1}{2} + \frac{i}{2\sqrt{4\mu^2-1}} & 0 \\ 0 & \frac{1}{2} - \frac{i}{2\sqrt{4\mu^2-1}} \end{pmatrix}, \quad \hat{\tau}_{0<\mu<\mu_c} = \begin{pmatrix} \frac{1}{2} + \frac{1}{2\sqrt{1-4\mu^2}} & 0 \\ 0 & \frac{1}{2} - \frac{1}{2\sqrt{1-4\mu^2}} \end{pmatrix}. \tag{73}$$

Accordingly, we can easily obtain $\bar{\tau} = \tilde{\tau}\tilde{\tau}^\dagger = \mathbb{I}/2$ in the PT-symmetric region. Furthermore, we compute the four entropies for both the PT-symmetric and PT-broken regions, and the results are displayed in Fig. 12, showing the entropy values as functions of μ.

As seen in the left panel of Fig. 12, in the PT-symmetric region, both pseudo and modified pseudo entropy are real. For large μ, they approach $\ln 2$. As μ decreases, the

pseudo entropy grows and diverges positively at the exceptional point. However, the modified pseudo entropy decreases, becomes negative, and diverges negatively at μ_c. In the PT-broken region, the modified pseudo entropy remains real and negative, while the pseudo entropy becomes complex. In the right panel, both SVD and ABB entropies take the real and positive values, and are strictly bounded by the logarithm of Hilbert space dimension in both the PT-symmetric and PT-broken regions. Notably, the SVD entropy is always larger than the ABB entropy in the PT-broken region.

We will see similar phenomena of entropies in SYK Lindbladian.

6.2 SYK Lindbladian

We now turn to the non-Hermitian vectorization of the Lindbladian superoperator in the SYK model.

In an isolated system without environmental interaction, the dynamics is governed by a Hermitian Hamiltonian, and ρ evolves according to the Heisenberg evolution: $d\rho/dt = -i[H,\rho]$. However, a truly isolated system is an idealization. In practice, a system is always coupled, to some degree, with an external environment. Under the assumption of weak coupling and in the Markovian limit, the open system dynamics is described by the Lindblad master equation [123],

$$\frac{d\rho}{dt} = \mathcal{L}(\rho), \quad \mathcal{L}(\rho) = -i[H,\rho] + \sum_{\alpha}\left(L_\alpha \rho L_\alpha^\dagger - \frac{1}{2}\{L_\alpha^\dagger L_\alpha, \rho\}\right), \tag{74}$$

where $\mathcal{L}$ is the Lindbladian superoperator, describing the non-unitary evolution of the system, H is the system's Hamiltonian, and L_α are jump operators encoding the interaction between the system and its environment.

The Lindbladian SYK models were proposed and investigated in [70, 124]. The SYK Hamiltonian incorporates the Gaussian-distributed random couplings [115],

$$H_{\mathrm{SYK}} = i^{q/2} \sum_{1\le i_1<\cdots<i_q\le N} J_{i_1\cdots i_q}\psi_{i_1}\cdots\psi_{i_q}, \tag{75}$$

where $\langle J_{i_1\cdots i_q}\rangle = 0$, $\langle J^2_{i_1\cdots i_q}\rangle = \frac{J^2(q-1)!}{N^{q-1}}$, and $\{\psi_i\}_{i=1}^N$ are Majorana fermionic operators satisfying $\{\psi_i,\psi_j\} = \delta_{ij}$. We choose the linear jump operators

$$L_i = \sqrt{\mu}\,\psi_i, \quad i = 1,2,\cdots,N. \tag{76}$$

where $\mu \ge 0$ is the strength of dissipation. Specifically, we refer to the following vectorized Lindbladian as non-Hermitian: it is the operator obtained by mapping the Lindbladian superoperator onto the double-copy Hilbert space $\mathcal{H}_a\otimes\mathcal{H}_b$ via the CJ isomorphism [71,72], and is given by [70]

$$\hat{\mathcal{L}} = -iH_a + i(-1)^{q/2}H_b - i\mu\sum_{i=1}^{N}\psi_{ai}\,\psi_{bi} - \mu\frac{N}{2}\mathbb{I}\,, \tag{77}$$

where $H_a = H_{\mathrm{SYK}}\otimes\mathbb{I}$ and $H_b = \mathbb{I}\otimes H_{\mathrm{SYK}}$, and ψ_{ai}, ψ_{bi} act on the double-copy Hilbert space, obeying $\{\psi_{si},\psi_{s'i'}\} = \delta_{ss'}\delta_{ii'}$, with $s,s'\in\{a,b\}$. The third term induced by the Lindblad terms describes the interaction between the systems a and b, corresponding to the two subspaces of $\mathcal{H}_a\otimes\mathcal{H}_b$, respectively. The Lindblad equation in superoperator form (74) can be mapped to $d\,|\rho\rangle\,/dt = \hat{\mathcal{L}}\,|\rho\rangle$ with $|\rho\rangle$ being the vectorization of ρ.

In this work, we define the PT symmetry of the vectorized Lindbladian in analogy with the definition used for non-Hermitian Hamiltonians in [121, 122], where the parity operator P is a unitary transformation and the time reversal operator T an anti-unitary one. The vectorized Lindbladian is PT-symmetric in the sense of

$$PT\hat{\mathcal{L}}(PT)^{-1} = \hat{\mathcal{L}}. \tag{78}$$

Further details of the vectorization and PT symmetry can be found in App. D. In this context, the PT symmetry of an eigenstate is preserved if its associated eigenvalue is real. Conversely, if the eigenvalue is complex, then the PT symmetry of the eigenstate is broken[4].

The spectrum of the vectorized Lindbladians (77) was computed numerically for finite N, revealing the complex eigenvalue distributions [70]. The real-time SYK Lindbladian dynamics was investigated in [129–132]. The symmetry classification of PT-symmetric SYK Lindbladians with more general Lindblad terms have also been investigated in [133, 134]. Various phenomena of non-Hermitian chaos have been studied in SYK Lindbladians, such as various form factors with dissipation [129, 135, 136] and dissipative scrambling [131, 132, 137, 138]. More recently, dissipative dynamics in bosonic SYK Lindbladian was studied in [139].

Here, we will numerically analyze the vectorized Lindbladian (77) and the PT symmetry breaking behavior of eigenstates for varying μ at $N = 8, q = 4$. Furthermore, we investigate the behavior of the four entropy measures associated with τ constructed from the bi-orthogonal eigenstates, with particular focus on the behavior near exceptional points.

We numerically calculate the spectrum of $\hat{\mathcal{L}}$ for the varying parameter μ within one disorder realization, shown in the left panel of Fig. 13, where we have omitted the last constant term in (77) as it merely induces a shift of the real parts of the spectrum along the real axis. For sufficiently large μ, the spectrum remains entirely real. As μ decreases, some pairs of eigenvalues approach each other, eventually colliding at some points, beyond which they become complex conjugate to each other. We trace two representative branches of eigenvalues that first undergo their transitions from $\{E_>, E_<\}$-branches to $\{E_+, E_-\}$-branches as μ decreases, as shown in the right panel of Fig. 13, where those branches of eigenvalues obey

$$\begin{aligned} &\mu > \mu_c: \quad E_>, E_< \in \mathbb{R}, \quad E_> > E_<; \\ &\mu = \mu_c: \quad E_< = E_> = E_+ = E_-; \\ &\mu < \mu_c: \quad E_+, E_- \in \mathbb{C}, \quad E_+^* = E_-. \end{aligned} \tag{79}$$

We present the spectrum for a single disorder realization and two representative branches in Fig. 13. Although different disorder realizations lead to different spectra, and different pairs of branches undergo the transition at different exceptional points, the qualitative nature of the transition and entropies is universal.

[4]However, the PT symmetry employed here differs from that introduced in [125], where the symmetry is defined in the superoperator space. In that framework, the PT transformation maps the Lindbladian $\mathcal{L} \to -\mathcal{L}$, leading to a distinct phase structure. For example, PT symmetry breaking typically occurs in the small μ region, in contrast to the behavior observed here. There are also other definitions of the PT symmetry with P and T defined in the operator space [126–128]. These framework also leads to the different phase structures. For example, in the PT-symmetric region, parts of the spectrum lie on the imaginary axis, while in the PT-broken region, all eigenvalues become real.

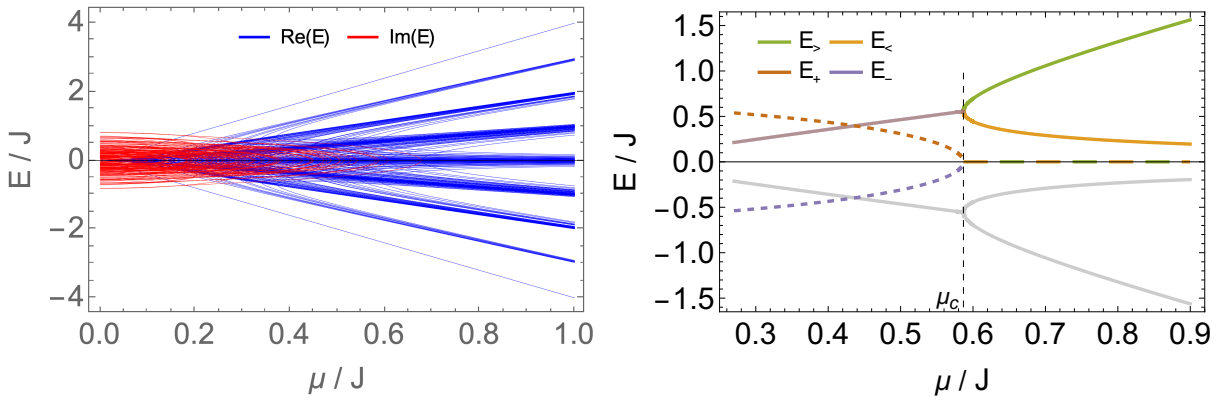

Figure 13: Left: Spectrum of the SYK Lindbladian for varying μ within a single disorder realization. Blue and red lines denote the real and imaginary parts, respectively. Right: Evolution of two branches of representative eigenvalues. Solid and dashed lines indicate the real and imaginary parts, respectively. In the PT-symmetric region, we label the upper positive branch (green) by $E_>$ and the lower positive branch (orange) by $E_<$. The two branches coincide at the exceptional point $\mu_c/J = 0.586$ and become a complex-conjugate pair in the PT-broken region. We label the branches with positive (brown) and negative (purple) imaginary parts by E_+ and E_-, respectively. In addition, we include the two branches (gray) that are additive inverses of the colored branches; they have the same entropies as their inverse counterparts.

Each eigenvalue corresponds to a left-right eigenstate pair in the bi-orthogonal basis. When $\mu > \mu_c$, the two corresponding eigenstates $\{|R_>\rangle, |R_<\rangle\}$ respect PT symmetry. At $\mu = \mu_c$, they coincide. When $\mu < \mu_c$, two new eigenstates $\{|R_+\rangle, |R_-\rangle\}$ are generated and do not respect PT-symmetry. So, for these two branches, we call (μ_c, ∞) the PT-symmetric region, μ_c the exceptional point, and $[0, \mu_c)$ the PT-broken region[5]

We then construct the transition matrices $\tau = \mathrm{Tr}_b |R\rangle \langle L|$ by tracing out the system b for each of right eigenstates $\{|R_>\rangle, |R_>\rangle\}$ or $\{|R_+\rangle, |R_-\rangle\}$ and their left counterparts. For each transition matrix in $\{\tau_<, \tau_>\}$ or $\{\tau_+, \tau_-\}$, we compute the (modified) pseudo entropy, the SVD entropy, and the ABB entropy.

The (modified) pseudo entropy is shown in Fig. 14. In the PT-symmetric region ($\mu > \mu_c$), the two branches of the pseudo entropy remain real and positive. As μ decreases, they increase and ultimately diverge at the exceptional point μ_c. The modified pseudo entropy for the branch $E_<$ decreases as μ decreases, eventually becomes negative, and diverges to $-\infty$ at μ_c, whereas for the branch $E_>$, it exhibits non-monotonic behavior and features a sharp increase in the vicinity of μ_c. In the PT-broken region ($\mu < \mu_c$), all (modified) pseudo entropies become complex and diverge at μ_c. Both branches E_+ and E_- share the same real part of the (modified) pseudo entropy, and their imaginary parts are additive inverses of each other.

The SVD and ABB entropies are shown in Fig. 15. Unlike the (modified) pseudo entropy, they remain real, positive, and strictly bounded by $\ln d_a = \frac{N}{2} \ln 2$. In the PT-symmetric region, the branch $E_>$ exhibits larger SVD and ABB entropies than the branch $E_<$. At μ_c, the entropies of each degenerate pair coincide and then decrease as μ is lowered further into the PT-broken region. These decreases are consistent with the tendency of the two eigenstates $\{|R_>\rangle, |R_<\rangle\}$ of the double-copy system to disentangle as the coupling

[5]Here, we define PT symmetry at the level of individual eigenstates, in contrast to the criterion in [121, 122], where a Hamiltonian is deemed PT-symmetric only if its entire spectrum is real.

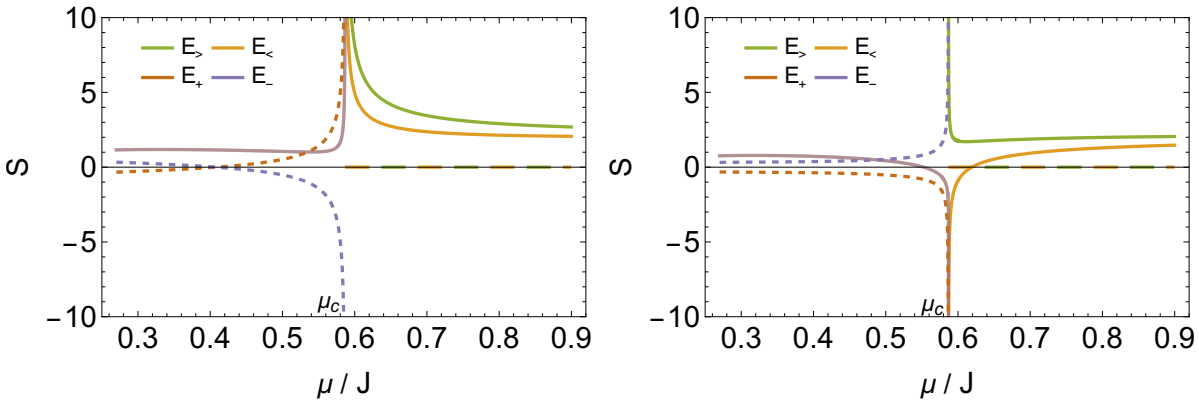

Figure 14: The pseudo entropy (left) and modified pseudo entropy (right) of τ constructed from the bi-orthogonal eigenstates along the two branches in the right panel of Fig. 13 in the same single realization.

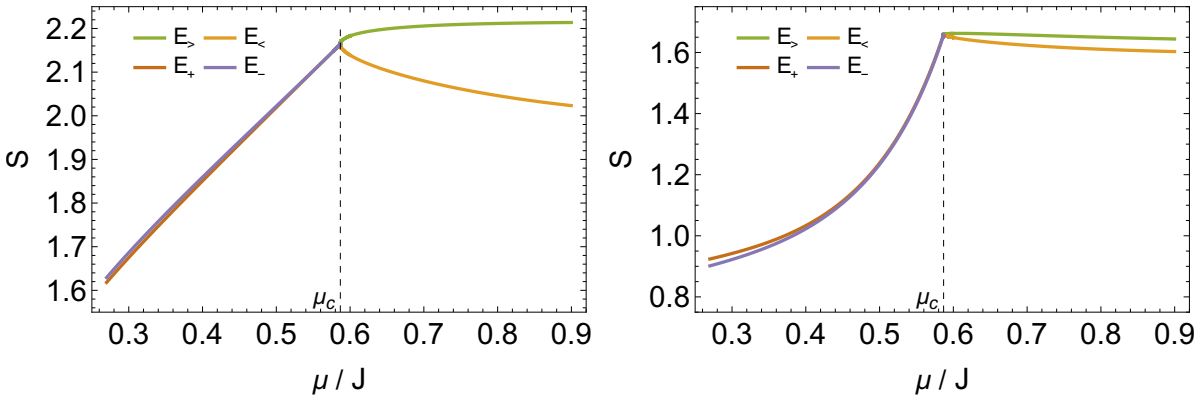

Figure 15: The SVD entropy (left) and ABB entropy (right) of the same τ in Fig.14.

μ is reduced. We also observe that the two branches take distinct values and that the SVD entropy is consistently greater than the ABB entropy for all μ.

Thus, we have shown that the divergence of the (modified) pseudo entropy challenges the claim that these entropies quantify quantum entanglement, even when they take real values. By contrast, both the SVD entropy and the ABB entropy behave consistently with the usual entanglement entropy of a single quantum state and align with the tendency toward disentanglement.

Finally, we observe some opposite monotonic behaviors of entropies, which also challenge the claim that (modified) pseudo entropy quantify quantum entanglement. For example, in the PT-symmetric region of the SYK Lindbladian, although all the four entropies of the $E_<$ branch are real, the monotonicity of the modified pseudo entropy as a function of μ is opposite to the monotonicity of others entropies. Similar situation happens in the PT-symmetric region of the two qubits system, where both the pseudo entropy and modified pseudo entropy change dramatically for varying μ but the SVD entropy and ABB entropy stay constant.

7 Conclusion and outlook

7.1 Conclusion

In this paper, we explored the transition matrix τ that describes a post-selection process transferring part of the information of a quantum state, either pure or mixed, from one side to another. In contrast to teleportation protocols, the transition matrix is not a trace-preserving map, due to post-selection. Hence, we employ entropy-based measures to quantify the amount of information transferred.

We introduced the ABB entropy of the transition matrix to quantify information transfer, which could be interpreted as the relative entropy between the input maximally mixed state and its output state bridged by the transition matrix (Sec. 2.2). The ABB entropy also avoids the issues encountered in the (modified) pseudo entropy and the SVD entropy. The pseudo entropy suffers from ambiguity due to the multi-valued logarithm. Both the pseudo and modified pseudo entropies can diverge or take complex values. Although the SVD entropy circumvents these problems, it lacks a clear probabilistic interpretation based on entanglement distillation of the two quantum states that construct the transition matrix (Sec. 3).

Subsequently, we demonstrated that the ABB entropy of the transition matrix does not increase under the addition of measurements and non-unitary operations, as illustrated in Fig. 3, in agreement with the behavior of conventional entanglement entropy for pure quantum states under LOCC [75]. By contrast, the (modified) pseudo entropy and the SVD entropy do not necessarily exhibit this monotonicity.

We showed that the ABB entropy of the large-copy transition matrices can be concentrated into that of the sub transition matrix with the highest probability (Sec. 3.2.1), following the notion of entanglement distillation in [67]. That probability corresponds to the highest probability of generalized measurement on a mixed state. We also examined the probabilistic interpretation of the pseudo and SVD entropies of the transition matrix in [12, 14]. We found that a meaningful concentration interpretation for the (modified) pseudo entropy is possible only when the normalized transition matrix has a real and non-negative spectrum, allowing them to be associated with a sub transition matrix. However, even in this case, the so-called "probability" of the concentration does not correspond to a true measurement probability in the quantum mechanical sense. For the transition matrices with negative or complex eigenvalues, it is even not possible to construct any probability-like distribution over the sub-transition matrices (Sec. 3.2.2). Similarly, for the SVD entropy, although the singular spectrum of the transition matrix is real and non-negative, the associated distribution over sub transition matrices still does not represent a genuine probability distribution in a quantum measurement process.

We computed the ensemble averages of the four entropies for transition matrices constructed from two independent Haar random states in Sec. 4, and from biorthogonal eigenstates of non-Hermitian random systems, including the GinUE and the non-Hermitian SYK model, in Sec. 5. In all cases, the SVD and ABB entropies exhibit behavior similar to the subsystem entanglement entropy of a single random state at large system size. By contrast, the pseudo entropy exceeds the constraint from the subsystem size and the modified pseudo entropy does not scale with subsystem size.

The contradistinction between these entropies becomes especially pronounced in a PT-symmetric model, as discussed in Sec. 6.2. Both the pseudo entropy and the modified pseudo entropy exhibit divergences near exceptional points and acquire complex values in the PT-broken region, while the SVD and ABB entropies remain finite in both the

PT-symmetric and PT-broken regions, and capture the entanglement properties of eigenstates.

7.2 Outlook

For two independent Haar random states, the subsystem-size asymmetry of the SVD and ABB entropies seen in Fig. 5 plausibly originates from subleading contributions in (63), so a detailed evaluation of these terms is warranted in future work. Moreover, while we numerically observe a plateau in the modified pseudo entropy in this case and attribute the emergence of negative values to spectral properties, an analytical computation of the spectrum for the normalized transition matrix remains for future investigation.

For bi-orthogonal states in the GinUE setting, although the SVD and ABB entropies exhibit Page-curve-like behavior in numerics, analytic expressions for them are still lacking, unlike the modified pseudo entropy, whose plateau is predictable [62]. Estimating their scaling behavior in future work would support a more compelling universal statement.

The ABB entropy has seen limited investigation in field-theoretic settings, and its structural properties remain largely unexplored. By contrast, pseudo entropy has been thoroughly studied in free scalar field theories and spin models [22, 23], where it displays area-law behavior, saturation, and the so-called non-positivity difference. In the biorthogonal basis of PT-symmetric systems, the pseudo and modified pseudo entropies exhibit logarithmic scaling with negative central charges at the critical points of the non-Hermitian spin and SSH models [13, 50, 59]. It remains an interesting question whether analogous behavior holds for the SVD and ABB entropies in such models.

Investigations of the ABB entropy within the framework of gravity duals are still lacking. For pseudo entropy, the corresponding transition matrix was realized in holographic framework [12, 37, 38]. A promising direction is to construct the gravity dual of the corresponding transition matrix for the ABB entropy in this setting.

Pseudo entropy is known to become complex in certain time-like configurations [39, 140], complicating its geometric interpretation [141]. In contrast, the SVD and ABB entropies remain real and positive even in time-evolved or non-unitary contexts, making it a potentially more robust alternative. Their construction also avoids ambiguities related to analytic continuation and partial swaps in imaginary time. Systematic exploration of its behavior under both unitary and non-unitary dynamics, could help establish SVD or ABB entropy as a potential diagnostic tool for temporal entanglement [142].

Acknowledgments

We are grateful to Zixia Wei, Giuseppe Di Giulio, and Jie Ping Zheng for helpful discussions. We are especially grateful to Zixia Wei for his detailed explanations and insightful suggestions on pseudo and SVD entropy. We are also indebted to Jonah Kudler-Flam for explanations of the numerical computations in the GinUE. R.M. and Z.-Y.X. acknowledge funding by DFG through the Collaborative Research Center SFB 1170 ToCoTronics, Project-ID 258499086-SFB 1170, as well as Germany's Excellence Strategy through the Würzburg-Dresden Cluster of Excellence on Complexity and Topology in Quantum Matter - ct.qmat (EXC 2147, project-id 390858490). Z.C. is financially supported by the China Scholarship Council. Z.-Y.X. also acknowledges support from the Berlin Quantum Initiative.

A Boundedness of ABB entropy by SVD entropy

In this appendix, we demonstrate that ABB entropy is always bounded by SVD entropy for a fixed transition matrix τ by proving $q \prec p$ rigorously. Let $Z_1 = \sum_{i=1}^{d} z_i$, $Z_2 = \sum_{i=1}^{d} z_i^2$ and arrange z_i in non-increasing order as $z_1 \geq \cdots \geq z_d$. For any $k \in \{1, \cdots, d\}$, define

$$\Delta_k := \sum_{i=1}^{k} q_i - \sum_{i=1}^{k} p_i = \frac{1}{Z_1} \sum_{i=1}^{k} z_i - \frac{1}{Z_2} \sum_{i=1}^{k} z_i^2. \tag{80}$$

Multiplying $Z_1 Z_2$ by Δ_k yields

$$\begin{aligned} Z_1 Z_2 \Delta_k &= Z_2 \sum_{i=1}^{k} z_i - Z_1 \sum_{i=1}^{k} z_i^2 = \sum_{j=1}^{d} \sum_{i=1}^{k} \left(z_j^2 z_i - z_j z_i^2 \right) \\ &= \sum_{i=1}^{k} \sum_{j=1}^{k} z_i z_j \left(z_j - z_i \right) + \sum_{i=1}^{k} \sum_{j=k+1}^{d} z_i z_j \left(z_j - z_i \right), \end{aligned} \tag{81}$$

where we split the sum over j into the parts of $j \leq k$ and $j > k$. The contribution of $j \leq k$ vanishes because the summand is anti symmetric under the exchange of i and j. Thus, only the term with $j > k$ survives:

$$Z_1 Z_2 \Delta_k = \sum_{i=1}^{k} \sum_{j=k+1}^{d} z_i z_j \left(z_j - z_i \right) \leq 0, \tag{82}$$

with the equality holding when $k = d$. Thus, $\Delta_k \leq 0$, i.e.,

$$\sum_{i=1}^{k} q_i \leq \sum_{i=1}^{k} p_i, \quad k = 1, \cdots, d. \tag{83}$$

As shown in Sec. 2.2, $S_{\mathrm{ABB}}[\tau] = S_{\mathrm{von}}(p)$ and $S_{\mathrm{SVD}}[\tau] = S_{\mathrm{von}}(q)$. Since the von Neumann entropy is Schur-concave, the majorization $q \prec p$ directly implies $S_{\mathrm{von}}(p) \leq S_{\mathrm{von}}(q)$, namely

$$S_{\mathrm{ABB}}[\tau] \leq S_{\mathrm{SVD}}[\tau], \tag{84}$$

with the equality holding iff all z_i are equal.

B Ensemble-averaged second Rényi ABB entropy over Haar random states

In the following, we present the detailed derivation of (58) and (59). We first reshape the states $|\psi_1\rangle_{bc} \in \mathcal{H}_b \otimes \mathcal{H}_c$ and $|\psi_2\rangle_{ab} \in \mathcal{H}_a \otimes \mathcal{H}_b$ into two matrices ψ and ϕ of dimensions $d_c \times d_b$ and $d_a \times d_b$, respectively. The corresponding expansions are expressed as $\psi = \sum_{i,j} \psi_{ij} |i\rangle_c \langle j|_b$ and $\phi = \sum_{i,j} \phi_{ij} |i\rangle_a \langle j|_b$. Thus, the transition matrix τ in (55) can be written as

$$\tau = \psi \phi^\dagger = \sum_{i=1}^{d_c} \sum_{k=1}^{d_a} \left(\sum_{j=1}^{d_b} \psi_{ij} \, \phi_{kj}^* \right) |i\rangle_c \langle k|_a , \tag{85}$$

whose components are $\tau_{ik} = \sum_j \psi_{ij}\,\phi^*_{kj}$ and $\left(\tau^\dagger\right)_{ki} = \sum_j \psi^*_{ij}\,\phi_{kj}$. We then have

$$\mathrm{Tr}\,\tau^\dagger\tau = \sum_{i=1}^{d_c}\sum_{k=1}^{d_a}\left(\sum_{j=1}^{d_b}\psi^*_{ij}\phi_{kj}\right)\left(\sum_{l=1}^{d_b}\psi_{il}\phi^*_{kl}\right) = \sum_{j,l=1}^{d_b}\left(\psi^\dagger\psi\right)_{jl}\left(\phi^\dagger\phi\right)_{lj} = \mathrm{Tr}\left(\psi^\dagger\psi\,\phi^\dagger\phi\right), \tag{86}$$

where $\psi^\dagger\psi = \mathrm{Tr}_c\,|\psi_1\rangle_{bc}\,\langle\psi_1|_{bc}$ and $\phi^\dagger\phi = \mathrm{Tr}_a\,|\psi_2\rangle_{ab}\,\langle\psi_2|_{ab}$ are both $d_b \times d_b$ dimensional matrices. The ensemble average of (86) over Haar random states, i.e., the case of $n = 1$ in (56), can be decomposed as

$$\overline{\mathrm{Tr}\,\tau^\dagger\tau} = \overline{\mathrm{Tr}\left(\psi^\dagger\psi\,\phi^\dagger\phi\right)} = \mathrm{Tr}\left[\overline{\psi^\dagger\psi}\;\overline{\phi^\dagger\phi}\right], \tag{87}$$

since U_{bc} and V_{ab} are drawn independently from two CUEs. Using the result of (57) for $k = 1$, we can obtain

$$\overline{\psi^\dagger\psi} = \mathrm{Tr}_c\overline{|\psi_1\rangle_{bc}\,\langle\psi_1|_{bc}} = \mathrm{Tr}_c\frac{I_{d_b}\otimes I_{d_c}}{d_b d_c} = \frac{I_{d_b}}{d_b}, \tag{88}$$

$$\overline{\psi^\dagger\psi} = \mathrm{Tr}_c\overline{|\psi_2\rangle_{ab}\,\langle\psi_2|_{ab}} = \mathrm{Tr}_a\frac{I_{d_a}\otimes I_{d_b}}{d_a d_b} = \frac{I_{d_b}}{d_b}, \tag{89}$$

where I_{d_a}, I_{d_b} and I_{d_c} are identity matrices of dimensions $d_a \times d_a$, $d_b \times d_b$ and $d_c \times d_c$. Therefore, we obtain

$$\overline{\mathrm{Tr}\,\tau^\dagger\tau} = \mathrm{Tr}_b\,\frac{I_{d_b}}{d_b^2} = \frac{1}{d_b}. \tag{90}$$

Next, we can express $\mathrm{Tr}\left[\left(\tau^\dagger\tau\right)^2\right]$ as

$$\begin{aligned}\mathrm{Tr}\left[\left(\tau^\dagger\tau\right)^2\right] &= \sum_{i_1,i_2,i_3,i_4=1}^{d_b}\left(\psi^\dagger\psi\right)_{i_1i_2}\left(\phi^\dagger\phi\right)_{i_2i_3}\left(\psi^\dagger\psi\right)_{i_3i_4}\left(\phi^\dagger\phi\right)_{i_4i_1}\\ &= \mathrm{Tr}\left(\psi^\dagger\psi\,\phi^\dagger\phi\,\psi^\dagger\psi\,\phi^\dagger\phi\right).\end{aligned} \tag{91}$$

Because U_{bc} and V_{ab} are independent, the ensemble average over Haar random states can be decomposed as

$$\overline{\mathrm{Tr}\left[\left(\tau^\dagger\tau\right)^2\right]} = \sum_{i_1,i_2,i_3,i_4=1}^{d_b}\overline{\left(\psi^\dagger\psi\right)^{\otimes 2}}_{i_1i_2;i_3i_4}\overline{\left(\phi^\dagger\phi\right)^{\otimes 2}}_{i_2i_3;i_4i_1} \tag{92}$$

Using the result of (57) for $k = 2$, we obtain

$$\overline{\left(\psi^\dagger\psi\right)^{\otimes 2}} = \mathrm{Tr}_c\overline{\left(|\psi_1\rangle_{bc}\,\langle\psi_1|_{bc}\right)^{\otimes 2}} = \frac{d_c^2\,I_{d_b}\otimes I_{d_b} + \mathrm{Tr}_c\,S_{(12)}}{d_b d_c(d_b d_c + 1)}, \tag{93}$$

where $S_{(12)}$ is the swap operator expanded as follows

$$S_{(12)} = \sum_{j,l=1}^{d_b}\sum_{i,k=1}^{d_c}|lk\rangle_1\otimes|ji\rangle_2\,\langle ji|_1\otimes\langle lk|_2\,. \tag{94}$$

Tracing out the system c yields $\mathrm{Tr}_c\, S_{(12)} = d_c \sum_{j,l} |l\rangle\langle j|_1 \otimes |j\rangle\langle l|_2$. So we have

$$\overline{(\psi^\dagger\psi)^{\otimes 2}}_{i_1 i_2; i_3 i_4} = \frac{d_c^2\,\delta_{i_1 i_2}\delta_{i_3 i_4} + d_c\,\delta_{i_1 i_4}\delta_{i_2 i_3}}{d_b d_c(d_b d_c + 1)}. \tag{95}$$

Similarly, we have

$$\overline{(\phi^\dagger\phi)^{\otimes 2}}_{i_2 i_3; i_4 i_1} = \frac{d_a^2\,\delta_{i_2 i_3}\delta_{i_4 i_1} + d_a\,\delta_{i_2 i_1}\delta_{i_3 i_4}}{d_a d_b(d_a d_b + 1)}. \tag{96}$$

Substituting (95) and (96) into (92) yields the result of (58). Analogously, for

$$\overline{\mathrm{Tr}\,[\tau^\dagger\tau]^2} = \sum_{i_1,i_2,i_3,i_4=1}^{d_b} \overline{(\psi^\dagger\psi)^{\otimes 2}}_{i_1 i_2; i_3 i_4}\,\overline{(\phi^\dagger\phi)^{\otimes 2}}_{i_2 i_1; i_4 i_3}, \tag{97}$$

we find

$$\overline{(\phi^\dagger\phi)^{\otimes 2}}_{i_2 i_1; i_4 i_3} = \frac{d_a^2\,\delta_{i_2 i_1}\delta_{i_4 i_3} + d_a\,\delta_{i_2 i_3}\delta_{i_1 i_4}}{d_a d_b(d_a d_b + 1)}, \tag{98}$$

and substituting (95) and (98) into (97) gives the result of (59).

C Proof of the symmetry and asymmetry of entropy measures in the ensemble average

In this appendix, we provide a detailed proof of the symmetry of the ensemble-averaged (modified) pseudo entropy and the asymmetry of the ensemble-averaged ABB and SVD entropy observed in Fig. 5, 7, 9 and 10. Consider two states $|\psi_1\rangle_{ab}$ and $|\psi_2\rangle_{ab}$ in a D-dimensional Hilbert space with $D = d_1 d_2$. The total Hilbert space is factorized as

$$\mathcal{H} = \mathcal{H}_a \otimes \mathcal{H}_b, \quad \dim \mathcal{H}_a = d_1, \quad \dim \mathcal{H}_b = d_2. \tag{99}$$

With respect to this partition, these two states can be expanded as

$$|\psi_1\rangle_{ab} = \sum_{i=1}^{d_1}\sum_{j=1}^{d_2} \psi_{ij}\,|i\rangle_a \otimes |j\rangle_b\,, \quad |\psi_2\rangle_{ab} = \sum_{i=1}^{d_1}\sum_{j=1}^{d_2} \phi_{ij}\,|i\rangle_a \otimes |j\rangle_b\,, \tag{100}$$

where $\{|i\rangle_a\}_{i=1}^{d_1}$ and $\{|j\rangle_b\}_{j=1}^{d_2}$ denote the two sets of orthonormal bases on d_1 and d_2-dimensional Hilbert spaces. It is convenient to reshape the coefficients as matrices $\psi = (\psi_{ij}) \in \mathbb{C}^{d_1\times d_2}$ and $\phi = (\phi_{ij}) \in \mathbb{C}^{d_1\times d_2}$, respectively.

Tracing out subsystem b yields the transition matrix τ_a, whose matrix elements are

$$(\tau_a)_{ik} = \sum_{j=1}^{d_2} \psi_{ij}\phi^*_{kj}, \tag{101}$$

or equivalently, $\tau_a = \psi\phi^\dagger \in \mathbb{C}^{d_1\times d_1}$. Similarly, tracing out subsystem a gives the transition matrix τ_b with components

$$(\tau_b)_{jl} = \sum_{i=1}^{d_1} \psi_{ij}\phi^*_{il}, \tag{102}$$

which can be written as $\tau_b = (\phi^\dagger\psi)^T \in \mathbb{C}^{d_2\times d_2}$.

Although τ_a and τ_b generally have different dimensions, the matrices $\psi\phi^\dagger$ and $\phi^\dagger\psi$ share the same nonzero eigenvalues with the same algebraic multiplicities. This is a standard linear-algebraic result: for $A \in \mathbb{C}^{m\times n}$ and $B \in \mathbb{C}^{n\times m}$, the matrices $AB \in \mathbb{C}^{m\times m}$ and $BA \in \mathbb{C}^{n\times n}$ have the identical nonzero spectra. A direct proof follows from the corollary of the Sylvester determinant theorem: assuming $m > n$,

$$\det(\lambda I_m - AB) = \lambda^{m-n}\det(\lambda I_n - BA). \tag{103}$$

For any $\lambda \neq 0$,

$$\det(\lambda I_m - AB) = \lambda^m \det\left(I_m - \frac{1}{\lambda}AB\right). \tag{104}$$

Now using the Sylvester determinant theorem: $\det(I_m + UV) = \det(I_n + VU)$ with $U = -\frac{1}{\lambda}A$ and $V = B$, one can get

$$\det\left(I_m - \frac{1}{\lambda}AB\right) = \det\left(I_n - \frac{1}{\lambda}BA\right). \tag{105}$$

Hence, substituting (105) into (104) yields

$$\det(\lambda I_m - AB) = \lambda^m \det\left(I_n - \frac{1}{\lambda}BA\right) = \lambda^{m-n}\det(\lambda I_n - BA). \tag{106}$$

Since both sides are polynomials in λ that agree for all $\lambda \neq 0$, the identity extends continuously to $\lambda = 0$. Consequently, AB and BA possess the same nonzero eigenvalues with the same algebraic multiplicities.

In the present setting, we identify $A = \psi$, $B = \phi^\dagger$, $m = d_1$, and $n = d_2$. Therefore, τ_a and τ_b share identical nonzero spectra. For a single realization of $|\psi_1\rangle_{ab}$ and $|\psi_2\rangle_{ab}$, this implies

$$S_{\mathrm{P}}[\tau_a] = S_{\mathrm{P}}[\tau_b], \quad S_{\mathrm{MP}}[\tau_a] = S_{\mathrm{MP}}[\tau_b]. \tag{107}$$

Moreover, since the ensemble from which $|\psi_1\rangle_{ab}$ and $|\psi_2\rangle_{ab}$ are drawn is invariant under exchange of the two subsystems, we have

$$\overline{S_{\mathrm{P}}[\tau_a(d_1;d_2)]} = \overline{S_{\mathrm{P}}[\tau_a(d_2;d_1)]}, \quad \overline{S_{\mathrm{MP}}[\tau_a(d_1;d_2)]} = \overline{S_{\mathrm{MP}}[\tau_a(d_2;d_1)]}. \tag{108}$$

Despite the fact that τ_a and τ_b share the same nonzero spectra, their products with their adjoints differ:

$$\tau_a\tau_a^\dagger = \psi\phi^\dagger\phi\psi^\dagger, \qquad \tau_b\tau_b^\dagger = (\psi^\dagger\phi\phi^\dagger\psi)^T. \tag{109}$$

These matrices are no longer related by the AB–BA structure and therefore do not, in general, share the same nonzero spectra. To illustrate this explicitly, consider the case $d_1 = 4$ and $d_2 = 3$, with $\psi, \phi \in \mathbb{R}^{4\times 3}$ given by

$$\psi = \begin{pmatrix} 0 & -1 & -1 \\ 0 & -1 & 1 \\ -1 & 0 & 0 \\ 1 & 1 & 1 \end{pmatrix}, \qquad \phi = \begin{pmatrix} -1 & 1 & 1 \\ -1 & 1 & 1 \\ -1 & 0 & 0 \\ 1 & 1 & -1 \end{pmatrix}. \tag{110}$$

Direct computation yields

$$\tau_a = \begin{pmatrix} -2 & -2 & 0 & 0 \\ 0 & 0 & 0 & -2 \\ 1 & 1 & 1 & -1 \\ 1 & 1 & -1 & 1 \end{pmatrix}, \qquad \tau_b = \begin{pmatrix} 2 & 1 & -1 \\ 3 & -1 & -3 \\ 1 & 1 & -1 \end{pmatrix}. \tag{111}$$

The spectra are

$$\mathrm{spec}(\tau_a) = \{2, -1+i, -1-i, 0\}, \tag{112}$$
$$\mathrm{spec}(\tau_b) = \{2, -1+i, -1-i\}, \tag{113}$$

confirming that τ_a and τ_b share the same nonzero eigenvalues. However,

$$\mathrm{spec}(\tau_a \tau_a^\dagger) = \{12, 4+2\sqrt{2}, 4-2\sqrt{2}, 0\}, \tag{114}$$
$$\mathrm{spec}(\tau_b \tau_b^\dagger) \approx \{24.61, 3.18, 0.20\}, \tag{115}$$

which are manifestly different.

In general, $\bar{\tau}_a$ and $\bar{\tau}_b$ possess different spectra, and the same holds for $\tilde{\tau}_a \tilde{\tau}_a^\dagger$ and $\tilde{\tau}_b \tilde{\tau}_b^\dagger$. Consequently, the ABB entropy and the SVD entropy of the transition matrix are generically asymmetric under exchange of the subsystems,

$$S_{\mathrm{ABB}}[\tau_a] \neq S_{\mathrm{ABB}}[\tau_b], \quad S_{\mathrm{SVD}}[\tau_a] \neq S_{\mathrm{SVD}}[\tau_b]. \tag{116}$$

After ensemble averaging, this asymmetry persists,

$$\overline{S_{\mathrm{ABB}}[\tau_a(d_1;d_2)]} \neq \overline{S_{\mathrm{ABB}}[\tau_a(d_2;d_1)]}, \quad \overline{S_{\mathrm{SVD}}[\tau_a(d_1;d_2)]} \neq \overline{S_{\mathrm{SVD}}[\tau_a(d_2;d_1)]}. \tag{117}$$

D Vectorization and PT symmetry of the SYK Lindbladian

Here we introduce the vectorization of the SYK Lindbladian via the CJ isomorphism and analyze its PT-symmetry, following [70, 130, 143].

The Hilbert space $\mathcal{H}$ of N Majorana fermions is in dimension $2^{N/2}$. We use the Jordan-Wigner transformation [144, 145] to yield the $(2^{N/2} \times 2^{N/2})$-dimensional matrix representation of the N Majorana fermion,

$$\begin{aligned} \psi_{2k-1} &= \frac{(-1)^{k-1}}{\sqrt{2}} \sigma_z^{\otimes(k-1)} \otimes \sigma_x \otimes \mathbb{I}^{\otimes(N/2-k)}, \\ \psi_{2k} &= \frac{(-1)^{k-1}}{\sqrt{2}} \sigma_z^{\otimes(k-1)} \otimes \sigma_y \otimes \mathbb{I}^{\otimes(N/2-k)}. \end{aligned} \tag{118}$$

For later convenience, we define a Hermitian chiral matrix $S = i^{N(N-1)/2} \prod_{i=1}^{N} \sqrt{2}\,\psi_i$, where the product of Majorana fermions is ordered sequentially from $i = 1$ to N, and S satisfies $\{S, \psi_i\} = 0$ and $S^2 = 1$.

To implement the CJ isomorphism, we introduce the 2^N-dimensional double-copy Hilbert space $\mathcal{H} \otimes \mathcal{H}$. We define $2N$ Majorana fermion operators $\{\psi_{ai}, \psi_{bi}\}_{i=1}^{N}$ acting on the double-copy Hilbert space as

$$\psi_{ai} = \psi_i \otimes S, \quad \psi_{bi} = \mathbb{I} \otimes \psi_i, \quad i = 1, \cdots, N, \tag{119}$$

which obey the anti-commutation relation $\{\psi_{si}, \psi_{s'i'}\} = \delta_{ss'}\delta_{ii'}$ with $s, s' \in \{a, b\}$.

To define a CJ isomorphism, we uniquely specify a MES

$$\mathbb{I} \to |0\rangle = \frac{1}{2^{N/4}} \sum_{j=1}^{2^{N/2}} |j\rangle \otimes |\tilde{j}\rangle \quad \text{with} \quad \langle 0|0\rangle = 1, \tag{120}$$

in the double-copy Hilbert space, by imposing the requirement

$$\psi_{ai} |0\rangle = -i\psi_{bi} |0\rangle , \quad \forall i. \tag{121}$$

The detailed construction of $|0\rangle$ can be seen in App. A of [130]. Then, the CJ isomorphism, as a map from the operator space on the single-copy Hilbert space to the double-copy Hilbert space, is defined as

$$O \to O \otimes \mathbb{I} |0\rangle , \quad \forall O. \tag{122}$$

Using this CJ isomorphism and denoting the image of the density matrix ρ as $|\rho\rangle = \rho \otimes \mathbb{I} |0\rangle$, we can demonstrate $\mathcal{L}(\rho) \to \hat{\mathcal{L}} |\rho\rangle$ with the vectorization (77) via

$$\begin{aligned} H\,\rho \to H\rho \otimes \mathbb{I} |0\rangle &= i^{q/2} J_{i_1 \cdots i_q} (\psi_{i_1} \otimes \mathbb{I}) \cdots (\psi_{i_q} \otimes \mathbb{I})(\rho \otimes \mathbb{I}) |0\rangle \qquad (123) \\ &= i^{q/2} J_{i_1 \cdots i_q} (\psi_{i_1} \otimes S) \cdots (\psi_{i_q} \otimes S) |\rho\rangle = i^{q/2} J_{i_1 \cdots i_q} \psi_{ai_1} \cdots \psi_{ai_q} |\rho\rangle = H_a |\rho\rangle , \\ \rho\, H \to \rho H \otimes \mathbb{I} |0\rangle &= i^{q/2} J_{i_1 \cdots i_q} (\rho \otimes \mathbb{I})(\psi_{i_1} \otimes S) \cdots (\psi_{i_q} \otimes S) |0\rangle \qquad (124) \\ &= i^{q/2} J_{i_1 \cdots i_q} (\rho \otimes \mathbb{I})(-i)^q (\mathbb{I} \otimes \psi_{i_1}) \cdots (\mathbb{I} \otimes \psi_{i_q}) |0\rangle = (-1)^{q/2} H_b |\rho\rangle , \\ \psi_i\, \rho\, \psi_i \to \psi_i\, \rho\, \psi_i \otimes \mathbb{I} |0\rangle &= (\psi_i \otimes S)(\rho \otimes \mathbb{I})(\psi_i \otimes S) |0\rangle = -i\psi_{ai}\psi_{bi} |\rho\rangle , \qquad (125) \\ \frac{1}{2}\left(\psi_i^\dagger \psi_i \rho + \rho \psi_i^\dagger \psi_i\right) \to \frac{N}{4} (\mathbb{I}\rho + \rho\mathbb{I}) \otimes \mathbb{I} |0\rangle &= \frac{N}{2} \mathbb{I} \otimes \mathbb{I} |\rho\rangle , \qquad (126) \end{aligned}$$

where we use the Einstein summation convention, and H_a and H_b are both SYK Hamiltonians with identical random couplings, as given in (75). One can also easily check $\hat{\mathcal{L}} |0\rangle = 0$.

Obviously, $\hat{\mathcal{L}}$ is non-Hermitian, i.e., $\hat{\mathcal{L}}^\dagger \neq \hat{\mathcal{L}}$, but it enjoys PT symmetry [134],

$$\hat{\mathcal{L}} = PT\hat{\mathcal{L}}(PT)^{-1}, \quad P = \exp\left(-i\frac{\pi}{2} \sum_{i=1}^{N} \psi_{ai} S_a \psi_{bi}\right), \quad T = QK, \tag{127}$$

where $S_a = S \otimes \mathbb{I}$, $Q = \prod_{i=1} \sqrt{2}\, \psi_{a(2i)} \prod_{k=1} \sqrt{2}\, \psi_{b(2k)}$, and K is complex conjugation in the matrix representation (118). The unitary operator P acts as a parity operator, while the anti-unitary operator T represents time reversal. It can be easily checked that $PP^\dagger = 1$, $T^2 = (-1)^{N/2}$. Using the anti-commutation relations, the operator P can be further simplified as

$$P = \prod_{i=1}^{N} \frac{1}{\sqrt{2}} (1 - 2i\psi_{ai} S_a \psi_{bi}) , \tag{128}$$

where the product is still ordered sequentially from $i = 1$ to N. Under the action of P, the transformations of Majorana fermions are given by

$$P\psi_{ai}P^{-1} = -iS_a\psi_{bi}, \quad P\psi_{bi}P^{-1} = -i\psi_{ai}S_a. \tag{129}$$

Similarly, the action of T is given by

$$TiT^{-1} = -i, \quad T\psi_{ai}T^{-1} = \psi_{ai}, \quad T\psi_{bi}T^{-1} = \psi_{bi}. \tag{130}$$

One can directly verify (127) via the above properties.

However, the eigenstates of $\hat{\mathcal{L}}$ do not necessarily respect PT symmetry unless the corresponding eigenvalues are real. This follows from

$$\hat{\mathcal{L}}\,|R\rangle = E\,|R\rangle \Rightarrow \hat{\mathcal{L}}PT\,|R\rangle = PT\hat{\mathcal{L}}(PT)^{-1}PT\,|R\rangle = PT\hat{\mathcal{L}}\,|R\rangle = E^*PT\,|R\rangle\,. \tag{131}$$

Thus, if the spectrum is real, the eigenstates remain invariant up to a phase factor under the PT transformation, which means that they satisfy the PT symmetry. Conversely, if the spectrum contains complex eigenvalues, the PT transformation just maps an eigenstate $|R\rangle$ to another state $PT\,|R\rangle$ with eigenvalue E^*. This establishes that the spectrum of $\hat{\mathcal{L}}$ is symmetric under complex conjugation.

References

[1] Y. Aharonov, P. G. Bergmann and J. L. Lebowitz, *Time Symmetry in the Quantum Process of Measurement*, Phys. Rev. **134**(6B), B1410 (1964), doi:10.1103/PhysRev.134.B1410.

[2] Y. Aharonov, D. Z. Albert and L. Vaidman, *How the result of a measurement of a component of the spin of a spin-1/2 particle can turn out to be 100*, Phys. Rev. Lett. **60**, 1351 (1988), doi:10.1103/PhysRevLett.60.1351.

[3] J. Bub and H. Brown, *Curious properties of quantum ensembles which have been both preselected and post-selected*, Phys. Rev. Lett. **56**, 2337 (1986), doi:10.1103/PhysRevLett.56.2337.

[4] G. T. Horowitz and J. M. Maldacena, *The Black hole final state*, JHEP **02**, 008 (2004), doi:10.1088/1126-6708/2004/02/008, `hep-th/0310281`.

[5] S. Lloyd and J. Preskill, *Unitarity of black hole evaporation in final-state projection models*, JHEP **08**, 126 (2014), doi:10.1007/JHEP08(2014)126, `1308.4209`.

[6] R. Bousso and D. Stanford, *Measurements without Probabilities in the Final State Proposal*, Phys. Rev. D **89**(4), 044038 (2014), doi:10.1103/PhysRevD.89.044038, `1310.7457`.

[7] I. Akal, T. Kawamoto, S.-M. Ruan, T. Takayanagi and Z. Wei, *Page curve under final state projection*, Phys. Rev. D **105**(12), 126026 (2022), doi:10.1103/PhysRevD.105.126026, `2112.08433`.

[8] C. H. Bennett, G. Brassard, C. Crépeau, R. Jozsa, A. Peres and W. K. Wootters, *Teleporting an unknown quantum state via dual classical and einstein-podolsky-rosen channels*, Phys. Rev. Lett. **70**, 1895 (1993), doi:10.1103/PhysRevLett.70.1895.

[9] S. Pirandola, J. Eisert, C. Weedbrook, A. Furusawa and S. L. Braunstein, *Advances in quantum teleportation*, Nature Photonics **9**(10), 641–652 (2015), doi:10.1038/nphoton.2015.154.

[10] A. Uhlmann, *The "transition probability" in the state space of a $*$-algebra*, Rept. Math. Phys. **9**(2), 273 (1976), doi:10.1016/0034-4877(76)90060-4.

[11] R. Jozsa, *Fidelity for Mixed Quantum States*, J. Mod. Opt. **41**(12), 2315 (1994), doi:10.1080/09500349414552171.

[12] Y. Nakata, T. Takayanagi, Y. Taki, K. Tamaoka and Z. Wei, *New holographic generalization of entanglement entropy*, Phys. Rev. D **103**(2), 026005 (2021), doi:10.1103/PhysRevD.103.026005, 2005.13801.

[13] Y.-T. Tu, Y.-C. Tzeng and P.-Y. Chang, *Rényi entropies and negative central charges in non-Hermitian quantum systems*, SciPost Phys. **12**(6), 194 (2022), doi:10.21468/SciPostPhys.12.6.194, 2107.13006.

[14] A. J. Parzygnat, T. Takayanagi, Y. Taki and Z. Wei, *SVD entanglement entropy*, JHEP **12**, 123 (2023), doi:10.1007/JHEP12(2023)123, 2307.06531.

[15] P. Calabrese and J. Cardy, *Entanglement entropy and conformal field theory*, J. Phys. A **42**, 504005 (2009), doi:10.1088/1751-8113/42/50/504005, 0905.4013.

[16] P. Calabrese and J. L. Cardy, *Entanglement entropy and quantum field theory*, J. Stat. Mech. **0406**, P06002 (2004), doi:10.1088/1742-5468/2004/06/P06002, hep-th/0405152.

[17] S. Ryu and T. Takayanagi, *Holographic derivation of entanglement entropy from AdS/CFT*, Phys. Rev. Lett. **96**, 181602 (2006), doi:10.1103/PhysRevLett.96.181602, hep-th/0603001.

[18] S. Ryu and T. Takayanagi, *Aspects of Holographic Entanglement Entropy*, JHEP **08**, 045 (2006), doi:10.1088/1126-6708/2006/08/045, hep-th/0605073.

[19] A. Lewkowycz and J. Maldacena, *Generalized gravitational entropy*, JHEP **08**, 090 (2013), doi:10.1007/JHEP08(2013)090, 1304.4926.

[20] X. Dong, A. Lewkowycz and M. Rangamani, *Deriving covariant holographic entanglement*, JHEP **11**, 028 (2016), doi:10.1007/JHEP11(2016)028, 1607.07506.

[21] V. E. Hubeny, M. Rangamani and T. Takayanagi, *A Covariant holographic entanglement entropy proposal*, JHEP **07**, 062 (2007), doi:10.1088/1126-6708/2007/07/062, 0705.0016.

[22] A. Mollabashi, N. Shiba, T. Takayanagi, K. Tamaoka and Z. Wei, *Pseudo Entropy in Free Quantum Field Theories*, Phys. Rev. Lett. **126**(8), 081601 (2021), doi:10.1103/PhysRevLett.126.081601, 2011.09648.

[23] A. Mollabashi, N. Shiba, T. Takayanagi, K. Tamaoka and Z. Wei, *Aspects of pseudoentropy in field theories*, Phys. Rev. Res. **3**(3), 033254 (2021), doi:10.1103/PhysRevResearch.3.033254, 2106.03118.

[24] T. Nishioka, T. Takayanagi and Y. Taki, *Topological pseudo entropy*, JHEP **09**, 015 (2021), doi:10.1007/JHEP09(2021)015, 2107.01797.

[25] S. He, Y.-X. Zhang, L. Zhao and Z.-X. Zhao, *Entanglement and pseudo entanglement dynamics versus fusion in CFT*, JHEP **06**, 177 (2024), doi:10.1007/JHEP06(2024)177, 2312.02679.

[26] S. He, J. Yang, Y.-X. Zhang and Z.-X. Zhao, *Pseudo entropy of primary operators in $T\overline{T}/J\overline{T}$-deformed CFTs*, JHEP **09**, 025 (2023), doi:10.1007/JHEP09(2023)025, 2305.10984.

[27] S. He, J. Yang, Y.-X. Zhang and Z.-X. Zhao, *Pseudoentropy for descendant operators in two-dimensional conformal field theories*, Phys. Rev. D **109**(2), 025014 (2024), doi:10.1103/PhysRevD.109.025014, 2301.04891.

[28] Y. Ishiyama, R. Kojima, S. Matsui and K. Tamaoka, *Notes on pseudo entropy amplification*, PTEP **2022**(9), 093B10 (2022), doi:10.1093/ptep/ptac112, 2206.14551.

[29] W.-z. Guo, S. He and Y.-X. Zhang, *On the real-time evolution of pseudo-entropy in 2d CFTs*, JHEP **09**, 094 (2022), doi:10.1007/JHEP09(2022)094, 2206.11818.

[30] K. Shinmyo, T. Takayanagi and K. Tasuki, *Pseudo entropy under joining local quenches*, JHEP **02**, 111 (2024), doi:10.1007/JHEP02(2024)111, 2310.12542.

[31] W.-z. Guo, Y.-z. Jiang and Y. Jiang, *Pseudo entropy and pseudo-Hermiticity in quantum field theories*, JHEP **05**, 071 (2024), doi:10.1007/JHEP05(2024)071, 2311.01045.

[32] W.-z. Guo, S. He and Y.-X. Zhang, *Constructible reality condition of pseudo entropy via pseudo-Hermiticity*, JHEP **05**, 021 (2023), doi:10.1007/JHEP05(2023)021, 2209.07308.

[33] J. Mukherjee, *Pseudo Entropy in U(1) gauge theory*, JHEP **10**, 016 (2022), doi:10.1007/JHEP10(2022)016, 2205.08179.

[34] F. Omidi, *Pseudo Rényi Entanglement Entropies For an Excited State and Its Time Evolution in a 2D CFT* (2023), 2309.04112.

[35] W.-z. Guo and J. Zhang, *Sum rule for the pseudo-Rényi entropy*, Phys. Rev. D **109**(10), 106008 (2024), doi:10.1103/PhysRevD.109.106008, 2308.05261.

[36] P. Caputa, B. Chen, T. Takayanagi and T. Tsuda, *Thermal pseudo-entropy*, JHEP **01**, 003 (2025), doi:10.1007/JHEP01(2025)003, 2411.08948.

[37] H. Kanda, M. Sato, Y.-k. Suzuki, T. Takayanagi and Z. Wei, *AdS/BCFT with brane-localized scalar field*, JHEP **03**, 105 (2023), doi:10.1007/JHEP03(2023)105, 2302.03895.

[38] H. Kanda, T. Kawamoto, Y.-k. Suzuki, T. Takayanagi, K. Tasuki and Z. Wei, *Entanglement phase transition in holographic pseudo entropy*, JHEP **03**, 060 (2024), doi:10.1007/JHEP03(2024)060, 2311.13201.

[39] K. Doi, J. Harper, A. Mollabashi, T. Takayanagi and Y. Taki, *Pseudoentropy in dS/CFT and Timelike Entanglement Entropy*, Phys. Rev. Lett. **130**(3), 031601 (2023), doi:10.1103/PhysRevLett.130.031601, 2210.09457.

[40] Z. Chen, *Complex-valued Holographic Pseudo Entropy via Real-time AdS/CFT Correspondence* (2023), 2302.14303.

[41] X. Jiang, P. Wang, H. Wu and H. Yang, *Timelike entanglement entropy in dS_3/CFT_2*, JHEP **08**, 216 (2023), doi:10.1007/JHEP08(2023)216, 2304.10376.

[42] K. Narayan and H. K. Saini, *Notes on time entanglement and pseudo-entropy*, Eur. Phys. J. C **84**(5), 499 (2024), doi:10.1140/epjc/s10052-024-12855-x, 2303.01307.

[43] K. Narayan, *de Sitter space, extremal surfaces, and time entanglement*, Phys. Rev. D **107**(12), 126004 (2023), doi:10.1103/PhysRevD.107.126004, 2210.12963.

[44] K. Narayan, *Further remarks on de Sitter space, extremal surfaces, and time entanglement*, Phys. Rev. D **109**(8), 086009 (2024), doi:10.1103/PhysRevD.109.086009, 2310.00320.

[45] J. S. Cotler, G. Gur-Ari, M. Hanada, J. Polchinski, P. Saad, S. H. Shenker, D. Stanford, A. Streicher and M. Tezuka, *Black Holes and Random Matrices*, JHEP **05**, 118 (2017), doi:10.1007/JHEP05(2017)118, [Erratum: JHEP 09, 002 (2018)], 1611.04650.

[46] K. Papadodimas and S. Raju, *Local Operators in the Eternal Black Hole*, Phys. Rev. Lett. **115**(21), 211601 (2015), doi:10.1103/PhysRevLett.115.211601, 1502.06692.

[47] K. Goto, M. Nozaki and K. Tamaoka, *Subregion spectrum form factor via pseudoentropy*, Phys. Rev. D **104**(12), L121902 (2021), doi:10.1103/PhysRevD.104.L121902, 2109.00372.

[48] S. He, P. H. C. Lau and L. Zhao, *Detecting quantum chaos via pseudo-entropy*, JHEP **06**, 056 (2025), doi:10.1007/JHEP06(2025)056, 2403.05875.

[49] D. C. Brody, *Biorthogonal quantum mechanics*, J. Phys. A **47**(3), 035305 (2013), doi:10.1088/1751-8113/47/3/035305, 1308.2609.

[50] P.-Y. Chang, J.-S. You, X. Wen and S. Ryu, *Entanglement spectrum and entropy in topological non-Hermitian systems and nonunitary conformal field theory*, Phys. Rev. Res. **2**(3), 033069 (2020), doi:10.1103/PhysRevResearch.2.033069, 1909.01346.

[51] R. Modak and B. P. Mandal, *Eigenstate entanglement entropy in a PT-invariant non-Hermitian system*, Phys. Rev. A **103**(6), 062416 (2021), doi:10.1103/PhysRevA.103.062416, 2102.01097.

[52] Y.-B. Guo, Y.-C. Yu, R.-Z. Huang, L.-P. Yang, R.-Z. Chi, H.-J. Liao and T. Xiang, *Entanglement entropy of non-Hermitian free fermions*, J. Phys. Condens. Matter **33**(47), 475502 (2021), doi:10.1088/1361-648X/ac216e, 2105.09793.

[53] W.-Z. Yi, Y.-J. Hai, R. Xiao and W.-Q. Chen, *Exceptional entanglement in non-Hermitian fermionic models* (2023), 2304.08609.

[54] H. Shimizu and K. Kawabata, *Complex entanglement entropy for complex conformal field theory*, Phys. Rev. B **112**(8), 085112 (2025), doi:10.1103/n578-ljd5, 2502.02001.

[55] H.-H. Lu and P.-Y. Chang, *Biorthogonal quench dynamics of entanglement and quantum geometry in PT-symmetric non-hermitian systems* (2025), 2507.20155.

[56] F. Rottoli, M. Fossati and P. Calabrese, *Entanglement Hamiltonian in the non-Hermitian SSH model*, J. Stat. Mech. **2024**(6), 063102 (2024), doi:10.1088/1742-5468/ad4860, 2402.04776.

[57] Q. Chen, S. A. Chen and Z. Zhu, *Weak ergodicity breaking in non-hermitian many-body systems*, SciPost Physics **15**(2), 052 (2023), doi:10.21468/SciPostPhys.15.2.052, 2202.08638.

[58] C.-T. Hsieh and P.-Y. Chang, *Relating non-Hermitian and Hermitian quantum systems at criticality*, SciPost Phys. Core **6**, 062 (2023), doi:10.21468/SciPostPhysCore.6.3.062, 2211.12525.

[59] M. Fossati, F. Ares and P. Calabrese, *Symmetry-resolved entanglement in critical non-Hermitian systems*, Phys. Rev. B **107**(20), 205153 (2023), doi:10.1103/PhysRevB.107.205153, 2303.05232.

[60] W. Tang, F. Verstraete and J. Haegeman, *Matrix product state fixed points of non-Hermitian transfer matrices*, Phys. Rev. B **111**(3), 035107 (2025), doi:10.1103/PhysRevB.111.035107, 2311.18733.

[61] P.-Y. Yang and Y.-C. Tzeng, *Entanglement Hamiltonian and effective temperature of non-Hermitian quantum spin ladders*, SciPost Phys. Core **7**, 074 (2024), doi:10.21468/SciPostPhysCore.7.4.074, 2409.17062.

[62] G. Cipolloni and J. Kudler-Flam, *Entanglement Entropy of Non-Hermitian Eigenstates and the Ginibre Ensemble*, Phys. Rev. Lett. **130**(1), 010401 (2023), doi:10.1103/PhysRevLett.130.010401, 2206.12438.

[63] L.-M. Chen, Y. Zhou, S. A. Chen and P. Ye, *Quantum Entanglement and Non-Hermiticity in Free-Fermion Systems*, Chin. Phys. Lett. **41**(12), 127302 (2024), doi:10.1088/0256-307X/41/12/127302, 2408.11652.

[64] J. Fullwood and A. J. Parzygnat, *On Dynamical Measures of Quantum Information*, Entropy **27**(4), 331 (2025), doi:10.3390/e27040331, 2306.01831.

[65] Z. Wu, A. J. Parzygnat, V. Vedral and J. Fullwood, *Quantum mutual information in time*, New J. Phys. **27**(6), 064504 (2025), doi:10.1088/1367-2630/adde7d, 2410.02137.

[66] P. Caputa, S. Purkayastha, A. Saha and P. Sułkowski, *Musings on SVD and pseudo entanglement entropies*, JHEP **11**, 103 (2024), doi:10.1007/JHEP11(2024)103, 2408.06791.

[67] C. H. Bennett, H. J. Bernstein, S. Popescu and B. Schumacher, *Concentrating partial entanglement by local operations*, Phys. Rev. A **53**, 2046 (1996), doi:10.1103/PhysRevA.53.2046.

[68] H.-K. Lo and S. Popescu, *Concentrating entanglement by local actions: Beyond mean values* (1997), quant-ph/9707038.

[69] O. Alter, P. O. Brown and D. Botstein, *Singular value decomposition for genome-wide expression data processing and modeling.*, Proceedings of the National Academy of Sciences of the United States of America **97 18**, 10101 (2000).

[70] A. Kulkarni, T. Numasawa and S. Ryu, *Lindbladian dynamics of the Sachdev-Ye-Kitaev model*, Phys. Rev. B **106**(7), 075138 (2022), doi:10.1103/PhysRevB.106.075138, 2112.13489.

[71] M.-D. Choi, *Completely positive linear maps on complex matrices*, Linear Algebra Appl. **10**(3), 285 (1975), doi:10.1016/0024-3795(75)90075-0.

[72] A. Jamiołkowski, *Linear transformations which preserve trace and positive semidefiniteness of operators*, Rept. Math. Phys. **3**, 275 (1972), doi:10.1016/0034-4877(72)90011-0.

[73] R. Couvreur, J. L. Jacobsen and H. Saleur, *Entanglement in nonunitary quantum critical spin chains*, Phys. Rev. Lett. **119**(4), 040601 (2017), doi:10.1103/PhysRevLett.119.040601, 1611.08506.

[74] W. K. Wootters and W. H. Zurek, *A single quantum cannot be cloned*, Nature **299**(5886), 802 (1982).

[75] M. A. Nielsen, *Conditions for a Class of Entanglement Transformations*, Phys. Rev. Lett. **83**, 436 (1999), doi:10.1103/PhysRevLett.83.436, quant-ph/9811053.

[76] Z. Van Herstraeten, M. G. Jabbour and N. J. Cerf, *Continuous majorization in quantum phase space*, Quantum **7**, 1021 (2023), doi:10.22331/q-2023-05-24-1021, 2108.09167.

[77] N. Koukoulekidis and D. Jennings, *Constraints on magic state protocols from the statistical mechanics of Wigner negativity*, npj Quantum Inf. **8**(1), 42 (2022), doi:10.1038/s41534-022-00551-1, 2106.15527.

[78] J. de Boer, G. Di Giulio, E. Keski-Vakkuri and E. Tonni, *Continuous majorization in quantum phase space for Wigner-positive states and proposals for Wigner-negative states*, Phys. Rev. A **112**(3), 032405 (2025), doi:10.1103/w561-h3z5, 2412.19698.

[79] A. W. Marshall, I. Olkin and B. C. Arnold, *Inequalities: theory of majorization and its applications*, Springer (1979).

[80] G. Vidal, *On the characterization of entanglement*, J. Mod. Opt. **47**, 355 (2000), doi:10.1080/09500340008244048, quant-ph/9807077.

[81] G. Vidal, D. Jonathan and M. A. Nielsen, *Approximate transformations and robust manipulation of bipartite pure-state entanglement*, Phys. Rev. A **62**, 012304 (2000), doi:10.1103/PhysRevA.62.012304.

[82] Y. Xin and R. Duan, *Conditions for entanglement transformation between a class of multipartite pure states with generalized schmidt decompositions*, Phys. Rev. A **76**, 044301 (2007), doi:10.1103/PhysRevA.76.044301.

[83] L. van Luijk, A. Stottmeister, R. F. Werner and H. Wilming, *Pure State Entanglement and von Neumann Algebras*, Commun. Math. Phys. **406**(12), 296 (2025), doi:10.1007/s00220-025-05465-5, 2409.17739.

[84] R. Bhatia, *Matrix analysis*, vol. 169, Springer Science & Business Media (2013).

[85] J. Watrous, *The theory of quantum information*, Cambridge university press (2018).

[86] J. E. Peajcariaac and Y. L. Tong, *Convex functions, partial orderings, and statistical applications*, Academic Press (1992).

[87] M. B. Plenio and S. S. Virmani, *An Introduction to Entanglement Theory*, Quant. Inf. Comput. **7**(1-2), 001 (2007), doi:10.1007/978-3-319-04063-9_8, quant-ph/0504163.

[88] F. J. Dyson, *Statistical theory of the energy levels of complex systems. I*, J. Math. Phys. **3**, 140 (1962), doi:10.1063/1.1703773.

[89] M. L. Mehta, *Random matrices*, vol. 142, Elsevier (2004).

[90] F. Haake, *Quantum signatures of chaos*, Springer (1991).

[91] D. N. Page, *Average entropy of a subsystem*, Phys. Rev. Lett. **71**, 1291 (1993), doi:10.1103/PhysRevLett.71.1291, gr-qc/9305007.

[92] D. N. Page, *Information in black hole radiation*, Phys. Rev. Lett. **71**, 3743 (1993), doi:10.1103/PhysRevLett.71.3743, hep-th/9306083.

[93] S. Sen, *Average entropy of a subsystem*, Phys. Rev. Lett. **77**, 1 (1996), doi:10.1103/PhysRevLett.77.1, hep-th/9601132.

[94] G. Penington, *Entanglement Wedge Reconstruction and the Information Paradox*, JHEP **09**, 002 (2020), doi:10.1007/JHEP09(2020)002, 1905.08255.

[95] A. Almheiri, N. Engelhardt, D. Marolf and H. Maxfield, *The entropy of bulk quantum fields and the entanglement wedge of an evaporating black hole*, JHEP **12**, 063 (2019), doi:10.1007/JHEP12(2019)063, 1905.08762.

[96] P. Hayden, S. Nezami, X.-L. Qi, N. Thomas, M. Walter and Z. Yang, *Holographic duality from random tensor networks*, JHEP **11**, 009 (2016), doi:10.1007/JHEP11(2016)009, 1601.01694.

[97] A. W. Harrow, *The Church of the Symmetric Subspace* (2013), 1308.6595.

[98] D. A. Roberts and B. Yoshida, *Chaos and complexity by design*, JHEP **04**, 121 (2017), doi:10.1007/JHEP04(2017)121, 1610.04903.

[99] Y. Gu, *Moments of Random Matrices and Weingarten Functions*, Master's thesis, Queen's University (2013).

[100] D. Weingarten, *Asymptotic Behavior of Group Integrals in the Limit of Infinite Rank*, J. Math. Phys. **19**, 999 (1978), doi:10.1063/1.523807.

[101] B. Collins, *Moments and cumulants of polynomial random variables on unitary groups, the Itzykson-Zuber integral, and free probability*, Int. Math. Res. Not. **2003**(17), 953 (2003), doi:10.1155/S107379280320917X.

[102] J. Ginibre, *Statistical Ensembles of Complex, Quaternion and Real Matrices*, J. Math. Phys. **6**, 440 (1965), doi:10.1063/1.1704292.

[103] S.-S. Byun and P. J. Forrester, *Progress on the study of the Ginibre ensembles I: GinUE* (2022), 2211.16223.

[104] D. Bernard and A. LeClair, *A classification of non-hermitian random matrices*, In *Statistical Field Theories*, pp. 207–214. Springer (2002).

[105] K. Kawabata, K. Shiozaki, M. Ueda and M. Sato, *Symmetry and Topology in Non-Hermitian Physics*, Phys. Rev. X **9**(4), 041015 (2019), doi:10.1103/PhysRevX.9.041015, 1812.09133.

[106] J. Feinberg and A. Zee, *NonHermitian random matrix theory: Method of Hermitean reduction*, Nucl. Phys. B **504**, 579 (1997), doi:10.1016/S0550-3213(97)00502-6, cond-mat/9703087.

[107] W. E. Arnoldi, *The principle of minimized iterations in the solution of the matrix eigenvalue problem*, Quarterly of applied mathematics **9**(1), 17 (1951).

[108] K. Kawabata, Z. Xiao, T. Ohtsuki and R. Shindou, *Singular-Value Statistics of Non-Hermitian Random Matrices and Open Quantum Systems*, PRX Quantum **4**(4), 040312 (2023), doi:10.1103/PRXQuantum.4.040312, 2307.08218.

[109] F. Roccati, F. Balducci, R. Shir and A. Chenu, *Diagnosing non-Hermitian many-body localization and quantum chaos via singular value decomposition*, Phys. Rev. B **109**(14), L140201 (2024), doi:10.1103/PhysRevB.109.L140201, 2311.16229.

[110] P. Nandy, T. Pathak and M. Tezuka, *Probing quantum chaos through singular-value correlations in the sparse non-Hermitian Sachdev-Ye-Kitaev model*, Phys. Rev. B **111**(6), L060201 (2025), doi:10.1103/PhysRevB.111.L060201, 2406.11969.

[111] P. Nandy, T. Pathak, Z.-Y. Xian and J. Erdmenger, *Krylov space approach to singular value decomposition in non-Hermitian systems*, Phys. Rev. B **111**(6), 064203 (2025), doi:10.1103/PhysRevB.111.064203, 2411.09309.

[112] M. Baggioli, K.-B. Huh, H.-S. Jeong, X. Jiang, K.-Y. Kim and J. F. Pedraza, *Singular value decomposition and its blind spot for quantum chaos in non-Hermitian Sachdev-Ye-Kitaev models*, Phys. Rev. D **111**(10), L101904 (2025), doi:10.1103/PhysRevD.111.L101904, 2503.11274.

[113] M. Prasad, S. H. Tekur, B. K. Agarwalla and M. Kulkarni, *Assessment of spectral phases of non-hermitian quantum systems through complex and singular values*, Phys. Rev. B **111**, L161408 (2025), doi:10.1103/PhysRevB.111.L161408.

[114] A. Kitaev, *A simple model of quantum holography*, talk at KITP, 2015, http://online.kitp.ucsb.edu/online/entangled15/kitaev/; http://online.kitp.ucsb.edu/online/entangled15/kitaev2/.

[115] J. Maldacena and D. Stanford, *Remarks on the Sachdev-Ye-Kitaev model*, Phys. Rev. D **94**(10), 106002 (2016), doi:10.1103/PhysRevD.94.106002, 1604.07818.

[116] C. Liu, X. Chen and L. Balents, *Quantum Entanglement of the Sachdev-Ye-Kitaev Models*, Phys. Rev. B **97**(24), 245126 (2018), doi:10.1103/PhysRevB.97.245126, 1709.06259.

[117] Y. Huang, Y. Tan and N. Y. Yao, *Deviations from maximal entanglement for eigenstates of the Sachdev-Ye-Kitaev model* (2024), 2409.07043.

[118] A. M. García-García, Y. Jia, D. Rosa and J. J. M. Verbaarschot, *Dominance of Replica Off-Diagonal Configurations and Phase Transitions in a PT Symmetric Sachdev-Ye-Kitaev Model*, Phys. Rev. Lett. **128**(8), 081601 (2022), doi:10.1103/PhysRevLett.128.081601, 2102.06630.

[119] R. Hamazaki, K. Kawabata, N. Kura and M. Ueda, *Universality classes of non-Hermitian random matrices*, Phys. Rev. Res. **2**(2), 023286 (2020), doi:10.1103/PhysRevResearch.2.023286.

[120] A. M. García-García, L. Sá and J. J. M. Verbaarschot, *Symmetry Classification and Universality in Non-Hermitian Many-Body Quantum Chaos by the Sachdev-Ye-Kitaev Model*, Phys. Rev. X **12**(2), 021040 (2022), doi:10.1103/PhysRevX.12.021040, 2110.03444.

[121] C. M. Bender and S. Boettcher, *Real spectra in nonHermitian Hamiltonians having PT symmetry*, Phys. Rev. Lett. **80**, 5243 (1998), doi:10.1103/PhysRevLett.80.5243, physics/9712001.

[122] A. Mostafazadeh, *Pseudo-hermiticity versus pt symmetry: The necessary condition for the reality of the spectrum of a non-hermitian hamiltonian*, Journal of Mathematical Physics **43**(1), 205–214 (2002), doi:10.1063/1.1418246.

[123] G. Lindblad, *On the Generators of Quantum Dynamical Semigroups*, Commun. Math. Phys. **48**, 119 (1976), doi:10.1007/BF01608499.

[124] L. Sá, P. Ribeiro and T. Prosen, *Lindbladian dissipation of strongly-correlated quantum matter*, Phys. Rev. Res. **4**(2), L022068 (2022), doi:10.1103/PhysRevResearch.4.L022068, 2112.12109.

[125] T. c. v. Prosen, $\mathbb{PT}$*-symmetric quantum liouvillean dynamics*, Phys. Rev. Lett. **109**, 090404 (2012), doi:10.1103/PhysRevLett.109.090404.

[126] P. Rabl, S. Rotter, P. Kirton and J. Huber, *Emergence of PT-symmetry breaking in open quantum systems*, SciPost Phys. **9**(4), 052 (2020), doi:10.21468/SciPostPhys.9.4.052, 2003.02265.

[127] Y. Nakanishi and T. Sasamoto, *PT phase transition in open quantum systems with Lindblad dynamics*, Phys. Rev. A **105**(2), 022219 (2022), doi:10.1103/PhysRevA.105.022219.

[128] Y. Nakanishi, R. Hanai and T. Sasamoto, *Continuous time crystals as a PT symmetric state and the emergence of critical exceptional points* (2024), 2406.09018.

[129] K. Kawabata, A. Kulkarni, J. Li, T. Numasawa and S. Ryu, *Dynamical quantum phase transitions in Sachdev-Ye-Kitaev Lindbladians*, Phys. Rev. B **108**(7), 075110 (2023), doi:10.1103/PhysRevB.108.075110, 2210.04093.

[130] A. M. García-García, L. Sá, J. J. M. Verbaarschot and J. P. Zheng, *Keldysh wormholes and anomalous relaxation in the dissipative Sachdev-Ye-Kitaev model*, Phys. Rev. D **107**(10), 106006 (2023), doi:10.1103/PhysRevD.107.106006, 2210.01695.

[131] J. Liu, R. Meyer and Z.-Y. Xian, *Operator size growth in Lindbladian SYK*, JHEP **08**, 092 (2024), doi:10.1007/JHEP08(2024)092, 2403.07115.

[132] A. M. García-García, J. J. M. Verbaarschot and J.-p. Zheng, *Lyapunov exponent as a signature of dissipative many-body quantum chaos*, Phys. Rev. D **110**(8), 086010 (2024), doi:10.1103/PhysRevD.110.086010, 2403.12359.

[133] K. Kawabata, A. Kulkarni, J. Li, T. Numasawa and S. Ryu, *Symmetry of Open Quantum Systems: Classification of Dissipative Quantum Chaos*, PRX Quantum **4**(3), 030328 (2023), doi:10.1103/PRXQuantum.4.030328, 2212.00605.

[134] A. M. García-García, L. Sá, J. J. M. Verbaarschot and C. Yin, *Toward a classification of PT-symmetric quantum systems: From dissipative dynamics to topology and wormholes*, Phys. Rev. D **109**(10), 105017 (2024), doi:10.1103/PhysRevD.109.105017, 2311.15677.

[135] Y.-N. Zhou, T.-G. Zhou and P. Zhang, *General properties of the spectral form factor in open quantum systems*, Front. Phys. (Beijing) **19**(3), 31202 (2024), doi:10.1007/s11467-024-1406-7, 2303.14352.

[136] J. Li, S. Yan, T. Prosen and A. Chan, *Spectral form factor in chaotic, localized, and integrable open quantum many-body systems* (2024), 2405.01641.

[137] B. Bhattacharjee, P. Nandy and T. Pathak, *Operator dynamics in Lindbladian SYK: a Krylov complexity perspective*, JHEP **01**, 094 (2024), doi:10.1007/JHEP01(2024)094, 2311.00753.

[138] B. Bhattacharjee, X. Cao, P. Nandy and T. Pathak, *Operator growth in open quantum systems: lessons from the dissipative SYK*, JHEP **03**, 054 (2023), doi:10.1007/JHEP03(2023)054, 2212.06180.

[139] Y. Liu, A. Kulkarni and S. Ryu, *Dissipative Dynamics and Symmetry Breaking in Bosonic Sachdev-Ye-Kitaev Lindbladian* (2025), 2508.04802.

[140] K. Doi, J. Harper, A. Mollabashi, T. Takayanagi and Y. Taki, *Timelike entanglement entropy*, JHEP **05**, 052 (2023), doi:10.1007/JHEP05(2023)052, 2302.11695.

[141] M. P. Heller, F. Ori and A. Serantes, *Geometric Interpretation of Timelike Entanglement Entropy*, Phys. Rev. Lett. **134**(13), 131601 (2025), doi:10.1103/PhysRevLett.134.131601, 2408.15752.

[142] A. Milekhin, Z. Adamska and J. Preskill, *Observable and computable entanglement in time* (2025), 2502.12240.

[143] X.-L. Qi and A. Streicher, *Quantum Epidemiology: Operator Growth, Thermal Effects, and SYK*, JHEP **08**, 012 (2019), doi:10.1007/JHEP08(2019)012, 1810.11958.

[144] P. Jordan and E. P. Wigner, *Über das paulische äquivalenzverbot*, Springer (1993).

[145] M. A. Nielsen *et al.*, *The fermionic canonical commutation relations and the jordan-wigner transform*, School of Physical Sciences The University of Queensland **59**, 75 (2005).